A new evaluation of ^{17}O system (preliminary)

Zhenpeng Chen[1], Libo Zhou[2], Yeying Sun[1], Tao Ye[3]

1 Physics Department, Tsinghua University, Beijing, China

2 Graduate School, China Academy of Engineering Physics, Beijing, China

3 Institute of Applied Physics and Computational Mathematics, Beijing, China

IAEA meeting, 8-12, November，2021

1 The reaction channels

For $n+^{16}O$, include 9 channels:

‘ $^{16}O(n,n_0)^{16}O_0$ ’ ‘ $^{16}O(n,n_1)^{16}O_1$ ’ ‘ $^{16}O(n,n_2)^{16}O_2$ ’
‘ $^{16}O(n,n_3)^{16}O_3$ ’ ‘ $^{16}O(n,n_4)^{16}O_4$ ’

‘ $^{16}O(n,\alpha_0)^{13}C_0$ ’ ‘ $^{16}O(n,\alpha_1)^{13}C_1$ ’ ‘ $^{16}O(n,\alpha_2)^{13}C_2$ ’
‘ $^{16}O(n,\alpha_3)^{13}C_3$ ’

For $\alpha+^{13}C$, include 9 *reverse* channels:

‘ $^{13}C(\alpha,\alpha_0)^{13}C_0$ ’ ‘ $^{13}C(\alpha,\alpha_1)^{13}C_1$ ’ ‘ $^{13}C(\alpha,\alpha_2)^{13}C_2$ ’
‘ $^{13}C(\alpha,\alpha_3)^{13}C_3$ ’

‘ $^{13}C(\alpha,n_0)^{16}O_0$ ’ ‘ $^{13}C(\alpha,n_1)^{16}O_1$ ’ ‘ $^{13}C(\alpha,n_2)^{16}O_2$ ’
‘ $^{13}C(\alpha,n_3)^{16}O_3$ ’ ‘ $^{13}C(\alpha,n_4)^{16}O_4$ ’

1 The reaction channels

And a *reduced* channel (used for 8 to 30 MeV), which represents the total contribution of other channels.

i) for inelastic scattering, the reduce channel has these channels:

$^{16}O(n,n_k)^{16}O_k$, k=5,6,7,…;

ii) for (n,α) :

$^{16}O(n,\alpha_k)^{13}C_k$, k=4,5,6,…, which emits only one α;

iii) and for the rest channels:

(n,p), (n,d), (n,2n), (n,t), &(n,others).

The relationship of cross sections

- **(n, tot)=(n, el)+(n, inl)+(n, α)+(n, Redu-rest),** which can be used to describe the experimental data of (n, tot);
- **(n, el)= (n, el)**, which can be used to describe the experimental data of neutron *elastic* scattering;
- **(n, inl)=(n,n_1)+(n,n_2)+(n,n_3)+(n,n_4)+(n, Redu-inl)**, which can be used to describe the experimental data of neutron total *inelastic* scattering, in EXFOR, only has this kind of data. **(n, Redu-inl)** represents inelastic scattering part in **(n, Redu-all);**
- **(n, α)=(n,α_0)+(n,α_1)+(n,α_2)+(n,α_3)+(n, Redu-α)**, which can be used to describe the experimental data of total (n,α), in EXFOR, only has this kind of data. **(n, Redu-α)** represents (n,α) part in **(n, Redu-all);**

2 The relationship of cross sections

- **(n, Redu-all)=(n, Redu-inl)+(n, Redu-α)+(n, Redu-rest)**, this formula explains that the total contribution of the reduced channel can be divided into three parts on the right; (n, Redu-all) is determined by fitting all data, (n, Redu-inl) is determined by fitting total non-elastic scattering data, and (n, Redu-α) is determined by fitting total (n, α) data.
- **(n, Redu-rest)=(n, p)+(n, d)+(n, 2n)+(n, t)+(n, other)**, in EXFOR, **(n, p), (n, d), (n, 2n), (n, t)** has a few data respectively, and the value of them are very small;
- **(α, n)= (α, n_0)+ (α, n_1)+ (α, n_2)+ (α, n_3)+ (α, Redu)**, which can be used to describe the experimental data of total **(α, n)**, in EXFOR, only has this kind of data.

Current situation of data fitting

- All the levels of ^{17}O listed in ‘**Table (1993TI07): Energy levels of ^{17}O**’ have been used. A total of 181 energy levels were used, and the parameters of all energy levels were determined by fitting experimental data.

- The energy range of experimental data is 1e-7 to 32 MeV. The current fitting for experimental data looks good.

- Refer to figures as follows:

3 Current situation of data fitting

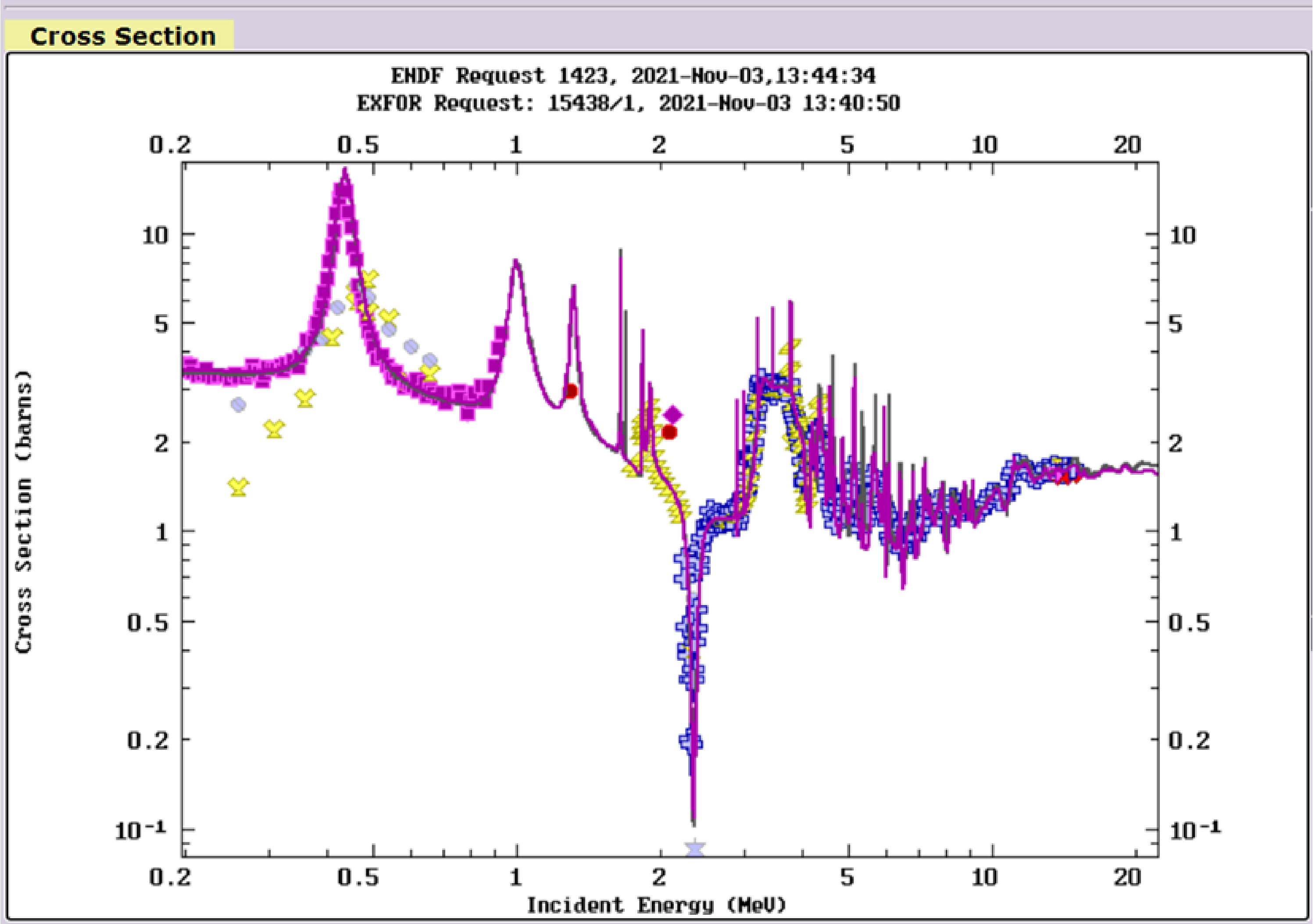

Figure1. The (n, tot) cross section, grey line represents ENDF/B8.0, purple line represents RAC2021. Below 20 MeV, they are very close. Above 20 MeV, there is a little difference, but this area lacks experimental data constraints. In this comprehensive fitting, the data of (n, tot) plays a dominant function.

3 Current situation of data fitting

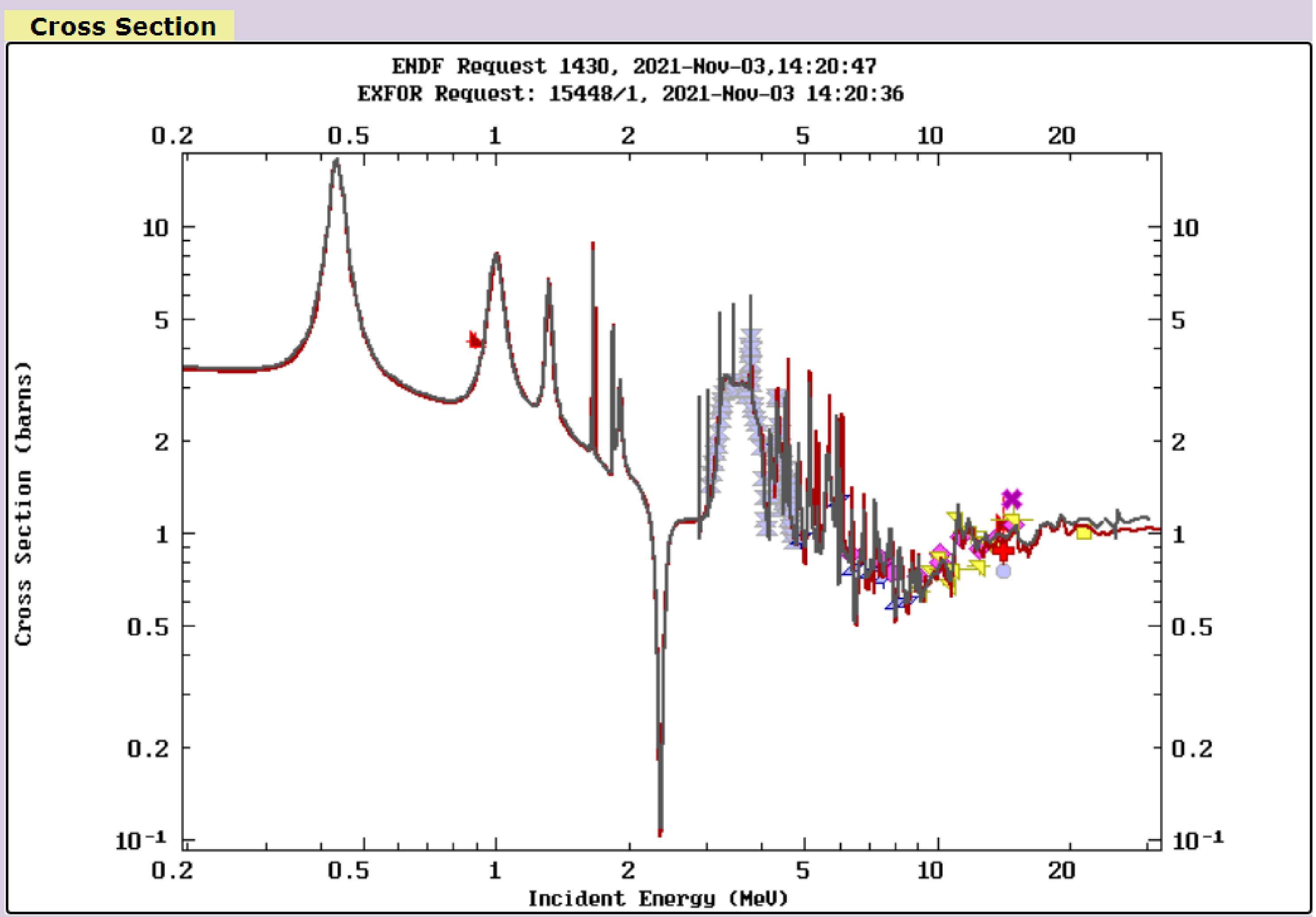

Figure2. The (n, el) scattering cross section, brown line represents ENDF/B8.0, grey line represents RAC2021. Below 20 MeV, they are very close, In this region, the elastic scattering differential cross section plays the decisive role, and the data fitting situation is shown in Appendix I. Above 20 MeV, there is a little difference, but this area lacks experimental data constraints.

3 Current situation of data fitting

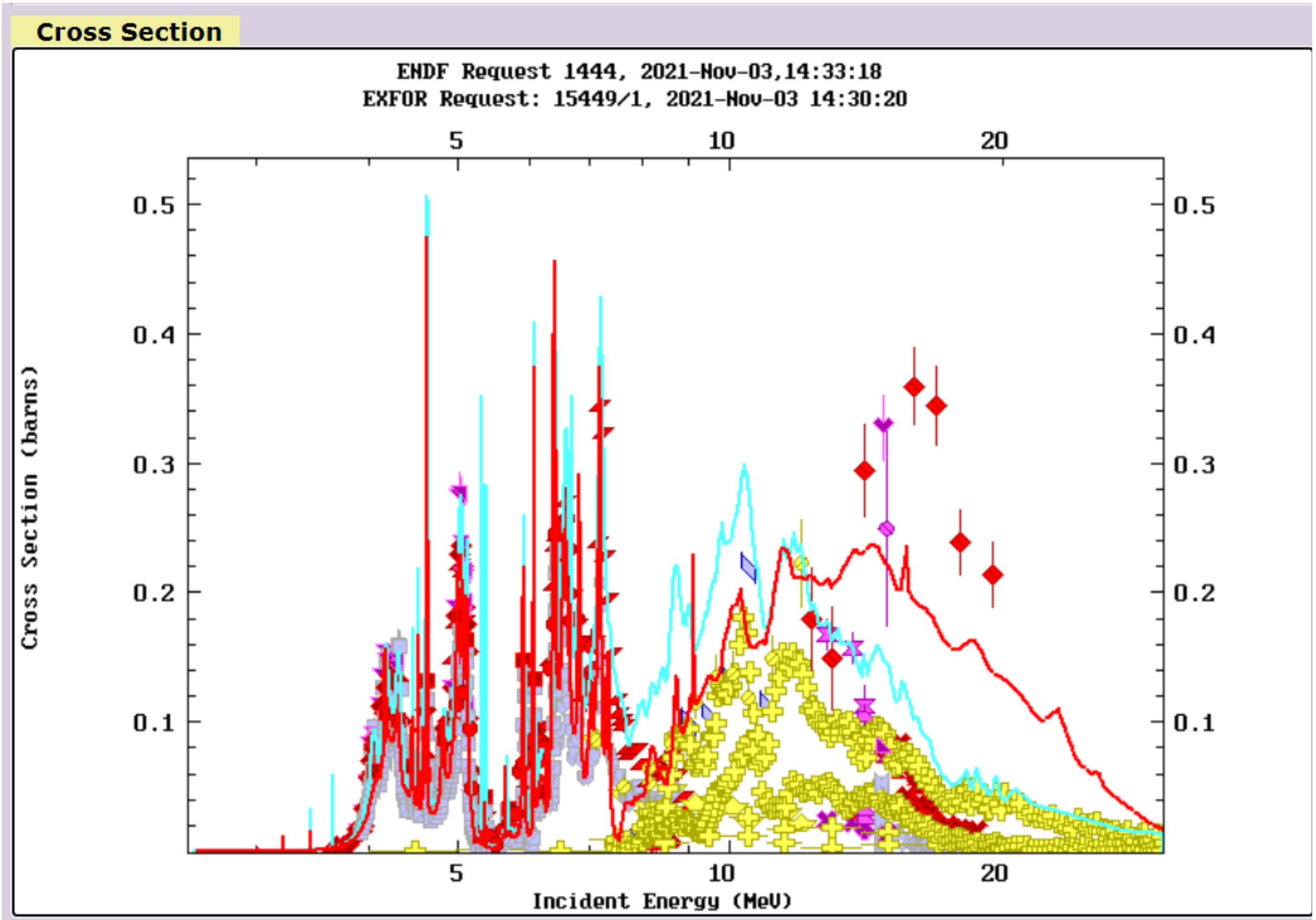

Figure3. The (n, α) cross section, blue line represents ENDF/B8.0, red line represents RAC2021. Below 7 MeV, they are close. In the 7 to 12 MeV range, there is a significant difference, but RAC2021 is closer to the experimental data. Above the 12MeV range, RAC2021 is significantly greater than ENDF/B8.0, and the experimental data of (n, α) have large differences. It should be emphasized here that in this kind of comprehensive evaluation, the fitting value of (n,α) depends on all experimental data instead of (n,α) data merely.

3 Current situation of data fitting

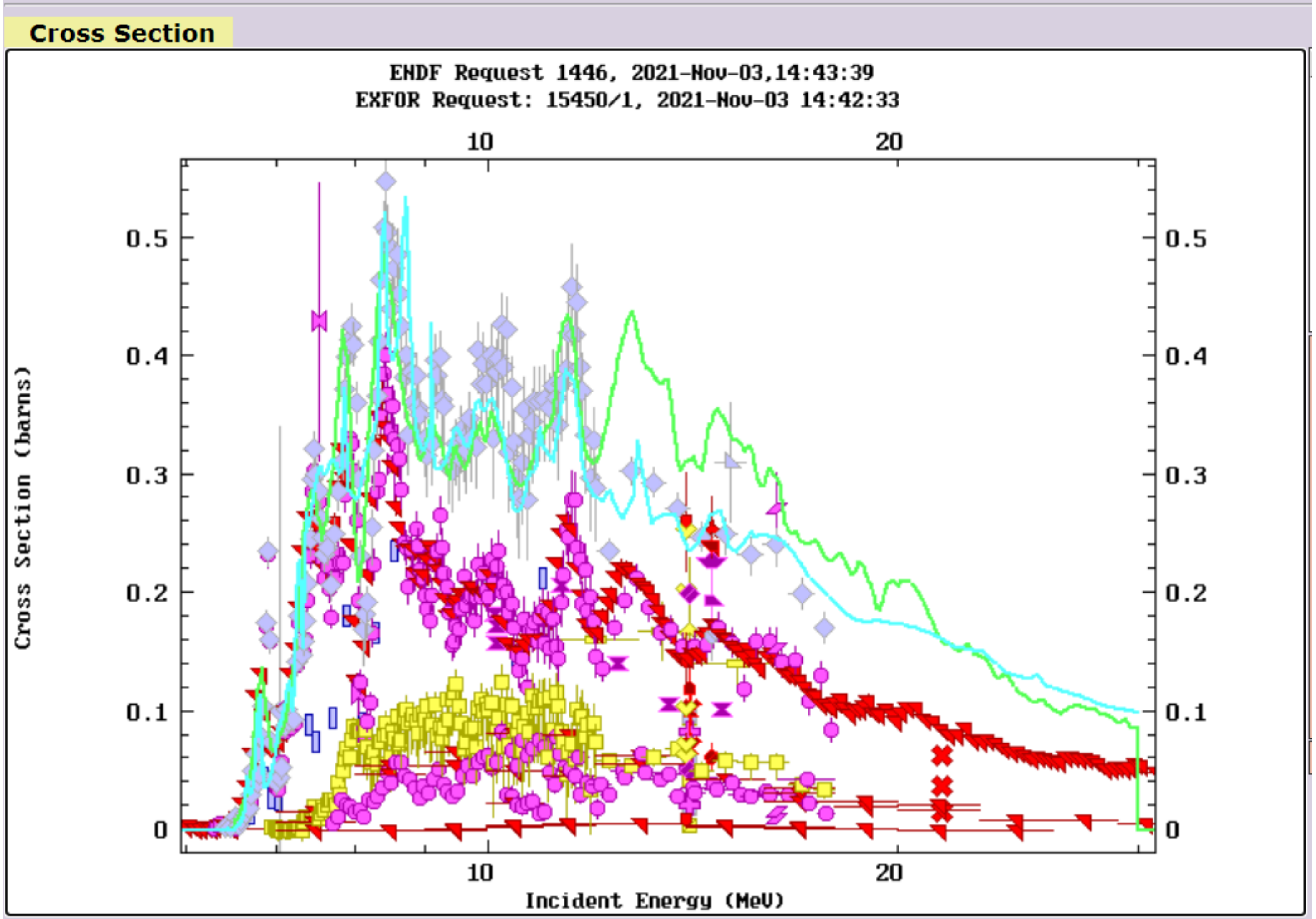

Figure4. The (n, inl) cross section, green line represents ENDF/B8.0, blue line represents RAC2021. Below 12 MeV, they are close. Above the 12MeV, there is a significant difference, but RAC2021 is closer to the latest experimental data (grey points), that is from Boromiza (2020) on (n, inl), which play a positive role of constraint and obvious improvement. It may have a positive effect on (n,α) and (α,n) evaluation improvement.

3 Current situation of data fitting

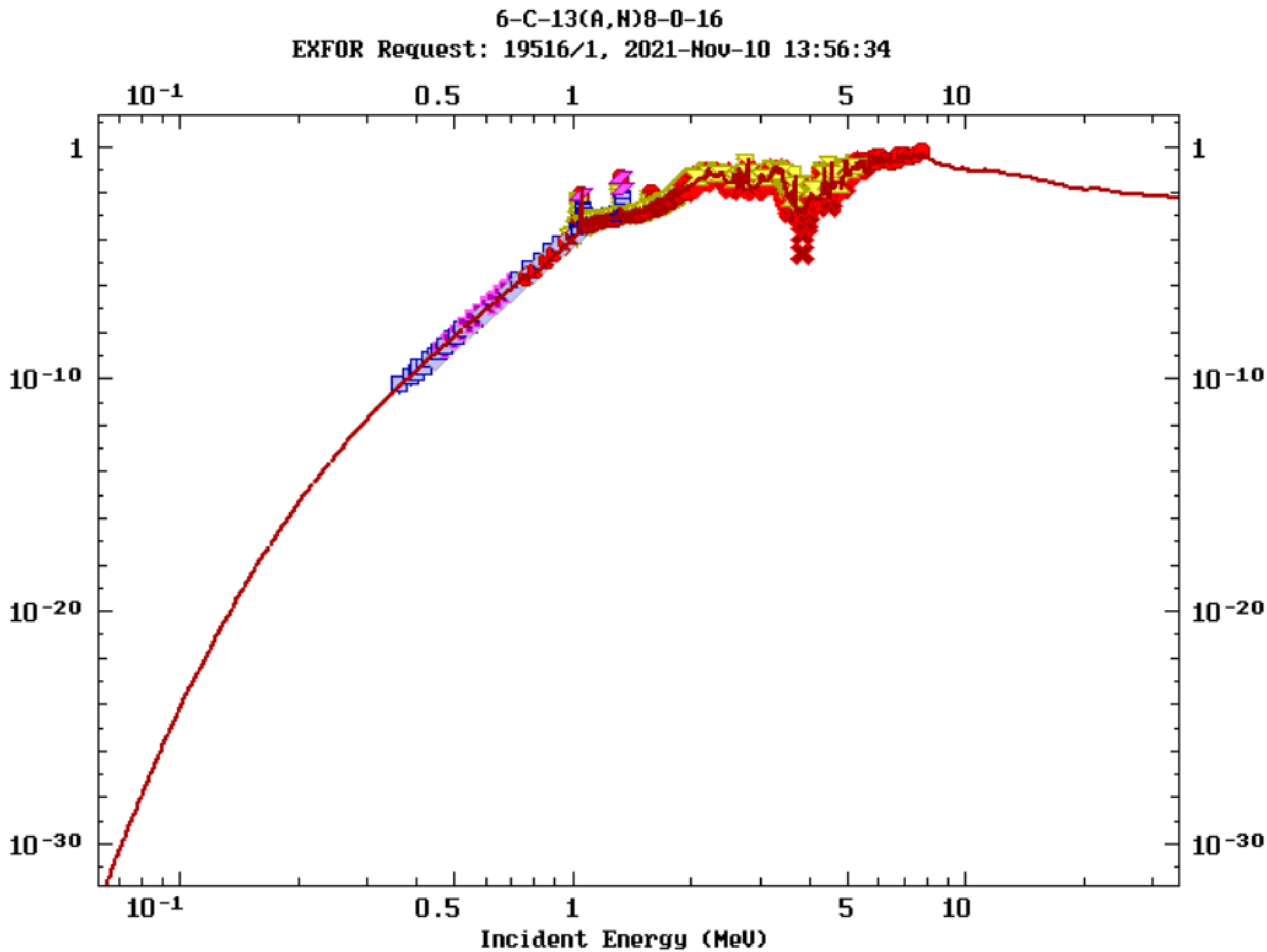

Figure5.1. The (α, n) cross section, no evaluation value can be found in ENDF files, red line represents RAC2021. Below 8 MeV, RAC2021 is very close to the experimental value. Above 8 MeV, the (α, n) evaluation depends on other data, especially (n, α) cross section.

3 Current situation of data fitting

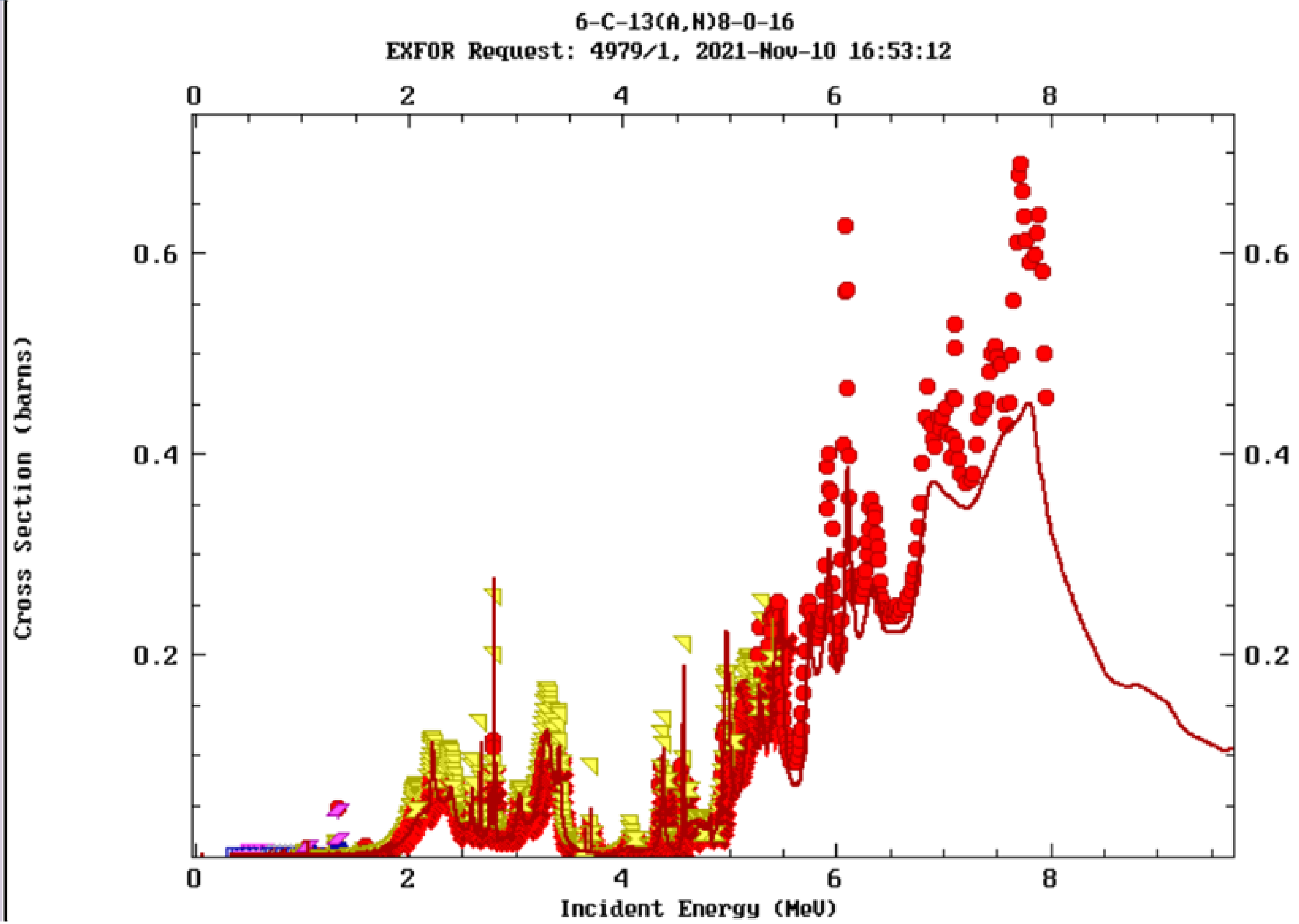

Figure5.2. The (α, n) cross section, no evaluation value can be found in ENDF files, red line represents RAC2021. Below 8 MeV, RAC2021 is very close to the experimental value. Above 8 MeV, the (α, n) evaluation depends on other data, especially (n, α) cross section.

4 Impact of new data on the evaluation

- The new evaluation process shows that, Boromiza (2020)'s new data on (n, inl) play a positive role of constraint and obvious improvement, which has been explained above, refer to Figure4;
- Gazeeva 2020's new data on (α, n0) (at 180 degree) has different shape with calculation value of RAC2021, refer to fig.6;

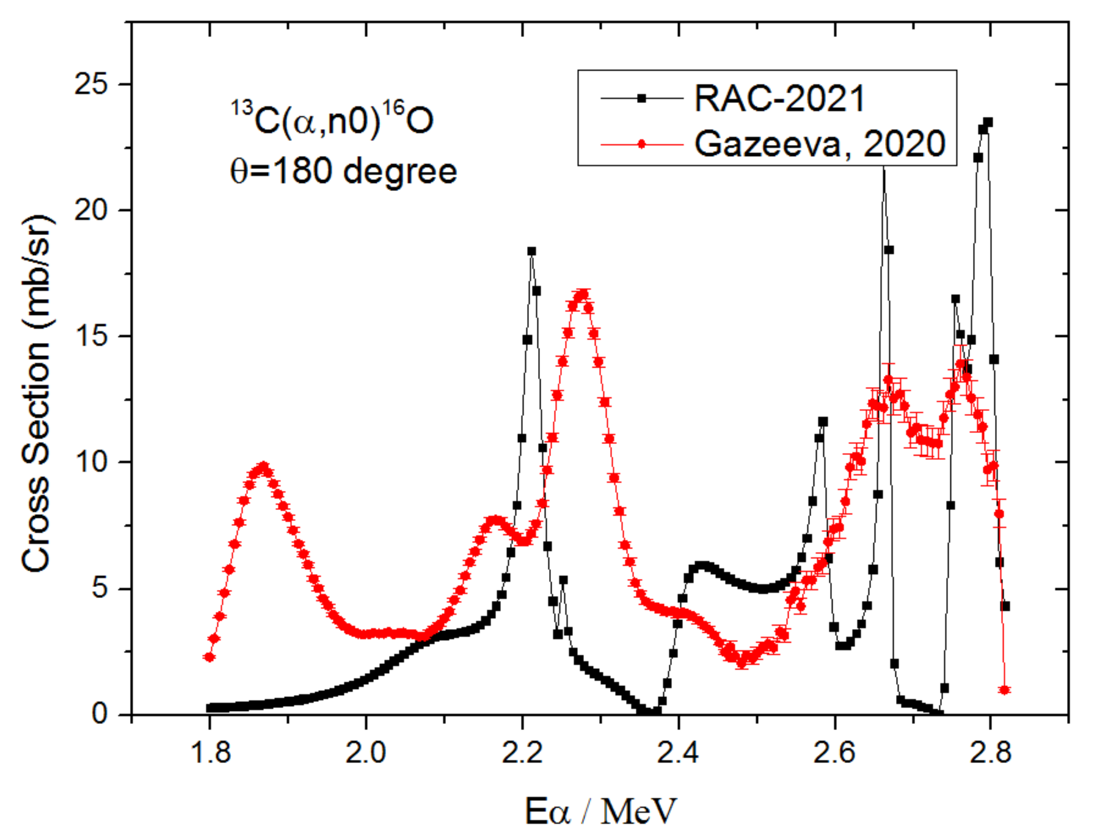

Figure6. Gazeeva 2020's new data.

4

Impact of new data on the evaluation

- The experimental data of deBoer have been transformed from the laboratory system to the center of mass system, where n and γ are considered approximately emitted in opposite directions. In deBoer's new data, (α, γ6130) plays a positive role of constraint and significant improvement, whose normalization coefficient is 1.000, refer to fig.7.

4 Impact of new data on the evaluation

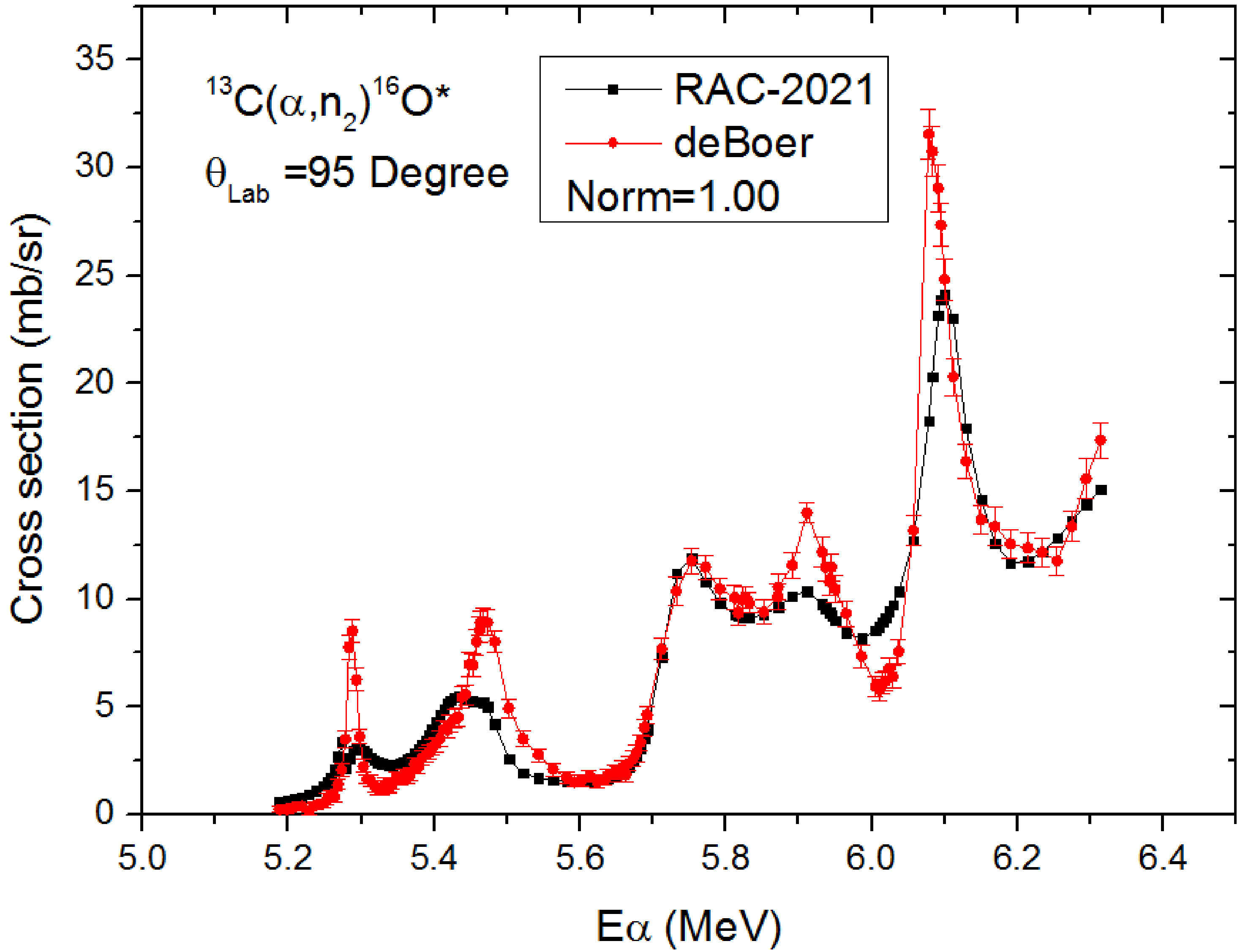

Figure7. deBoer's new data, (α, γ6130). Both peaks and amplitudes are agree with the calculation value of RAC2021.

Impact of new data on the evaluation

- The deBoer's differential cross section of (α, n0) plays a positive role of constraint. Refer to fig.8.

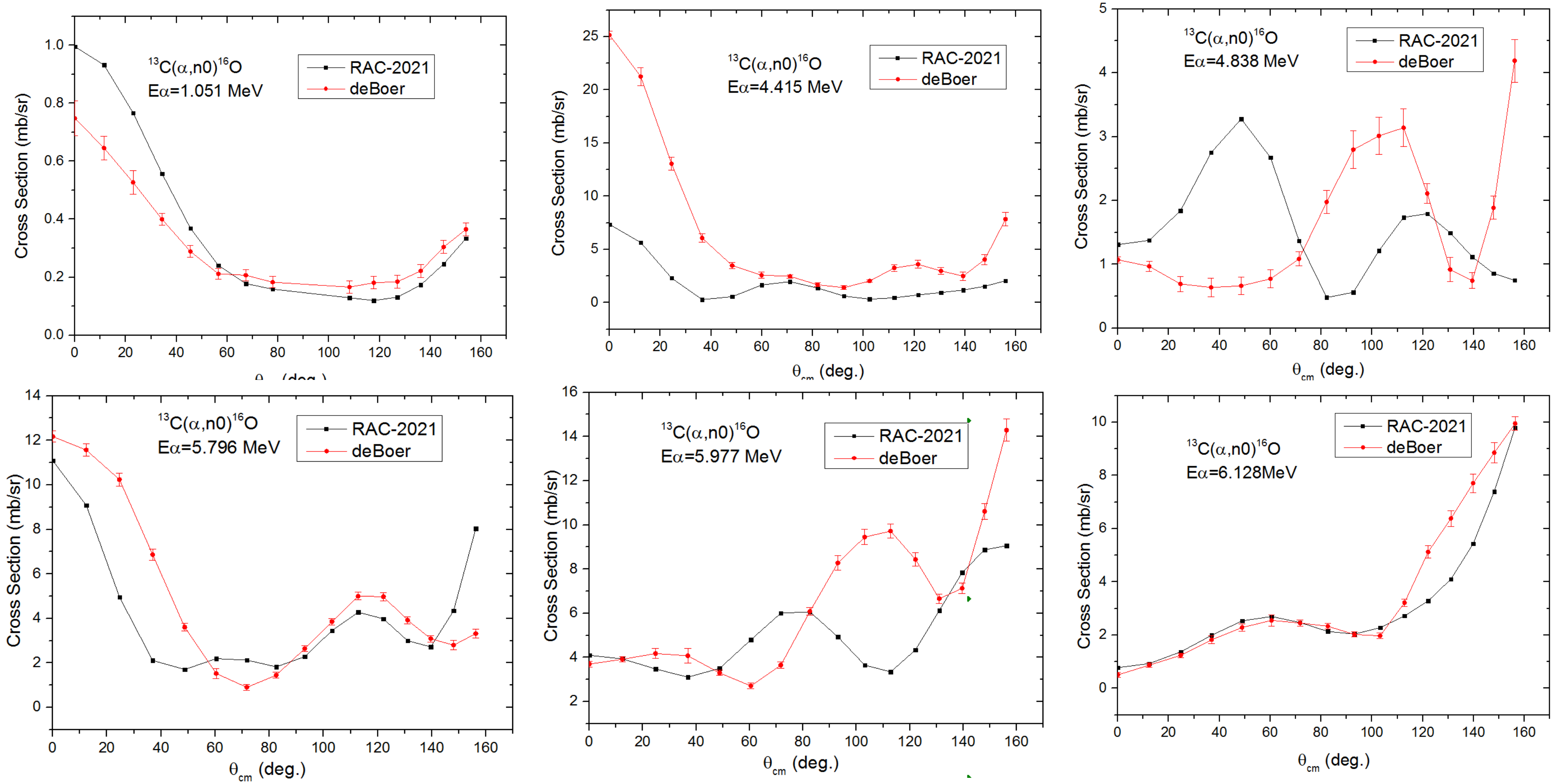

Figure8. deBoer's differential cross section of (α, n0) at 6 energies, all normalization coefficients are 1.0.

4 Impact of new data on the evaluation

- But, in Dr. deBoer's new data, the (α, γ6050) and all other data on (α, n1) are difficult to use. It looks too large to get good fitting, unless using very small (about 0.0025) normalization coefficient. We have tried to change the energy level properties in the corresponding energy region, but can't solve the problem. It looks that the experiment data of (n,tot) played a strong restraint role. There seems to be a big contradiction between this kind of data and the total cross-section.

4 Impact of new data on the evaluation

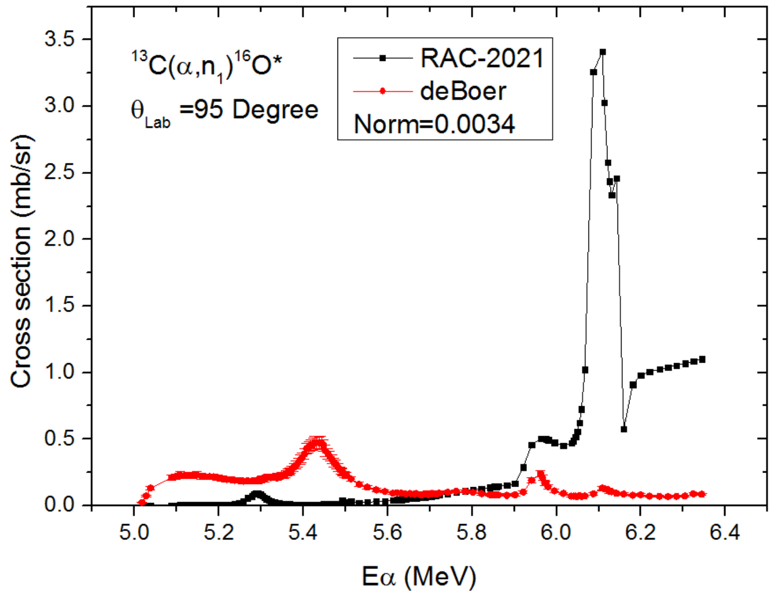

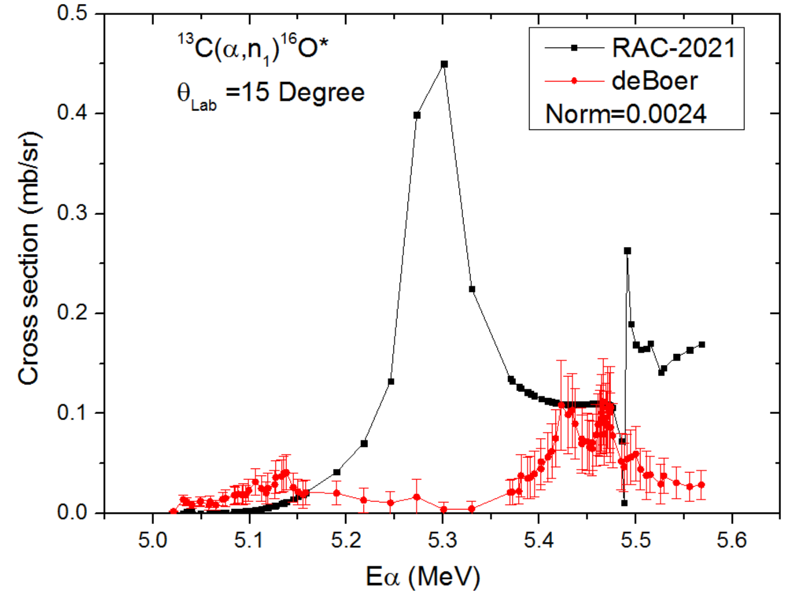

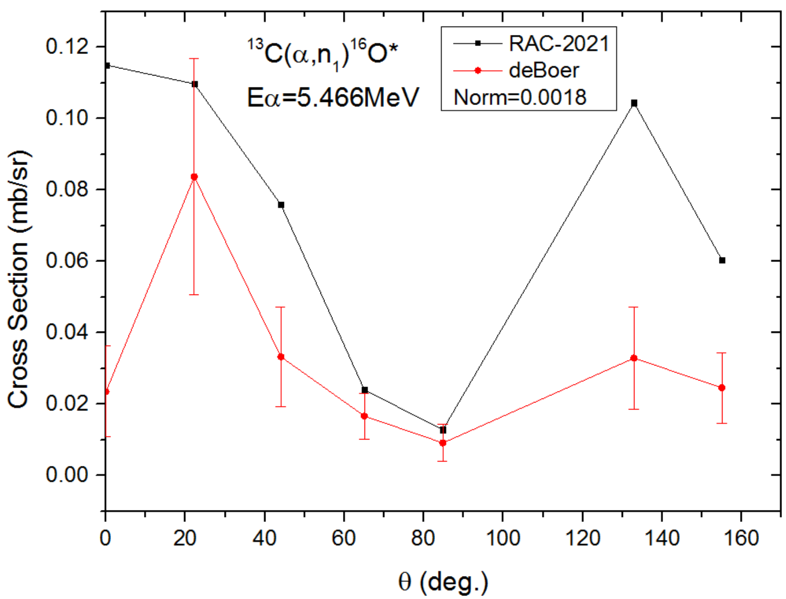

Figure9. The deBoer's data on (α, n1) are difficult to use. Notice that the normalization coefficients are very small (about 0.0025).

4 Impact of new data on the evaluation

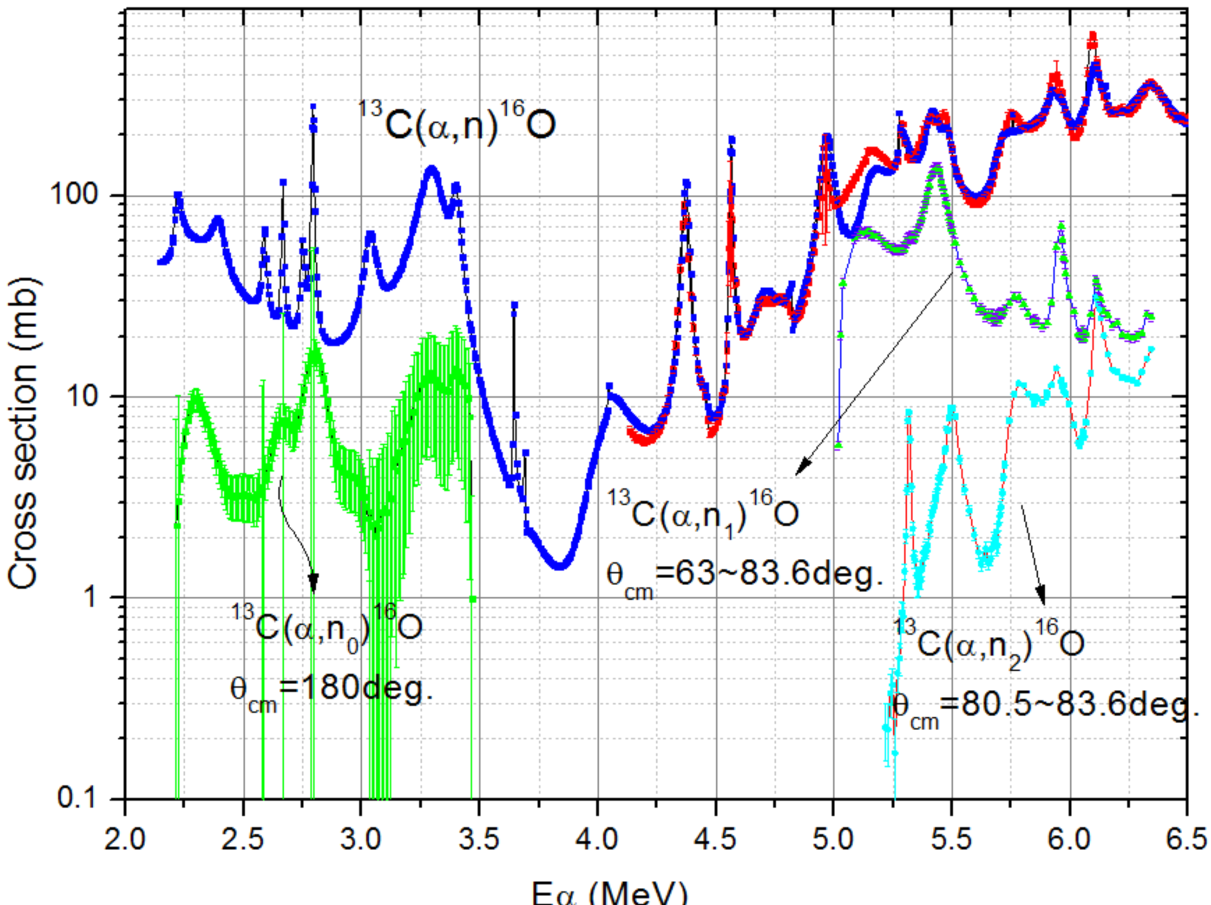

Figure10. The blue line and red line represent total (α, n) cross section. Through comparison with the curve of (α, n), it can be seen that both the positions and amplitudes of peaks in $^{13}C(\alpha, n2)^{16}O$ (blue points) are reasonable (refer to Fig.7). But for $^{13}C(\alpha, n1)^{16}O$, the positions of peaks look reasonable, while the amplitudes are unreasonable, eg., the peak near 5.4 MeV maybe too high, which should be lower than the peaks in higher energy.

4 Impact of new data on the evaluation

- Theoretically, the ground state of 16O is 0+, the first excited state (6050) is 0-, and the second excited state (6130) is 3-. So for gamma transitions, 0- to 0+ is forbidden, 3- to 0+ is open. So, (n, n2) is much larger than (n, n1), as the evaluation values in ENDF-B7 and RAC2021. And (α, n2) should be much larger than (α, n1), the (α, γ6130) should be larger than (α, γ6050), However, in deBoer's data, it's just the other way around, the (α, γ6050) is much larger than (α, γ6130), which requires careful study of the reasons why.

5 Set of integral C-S calculation values

- The calculated integral cross section includes: (n, tot), (n, el), (n, inl), (n, n1), (n, n2), (n, n3), (n, n4), (n, α0), (n, α1), (n, α2), (n, α3), (n, α4), (α, n), (α, n0), (α, n1), (α, n2), (α, n3).

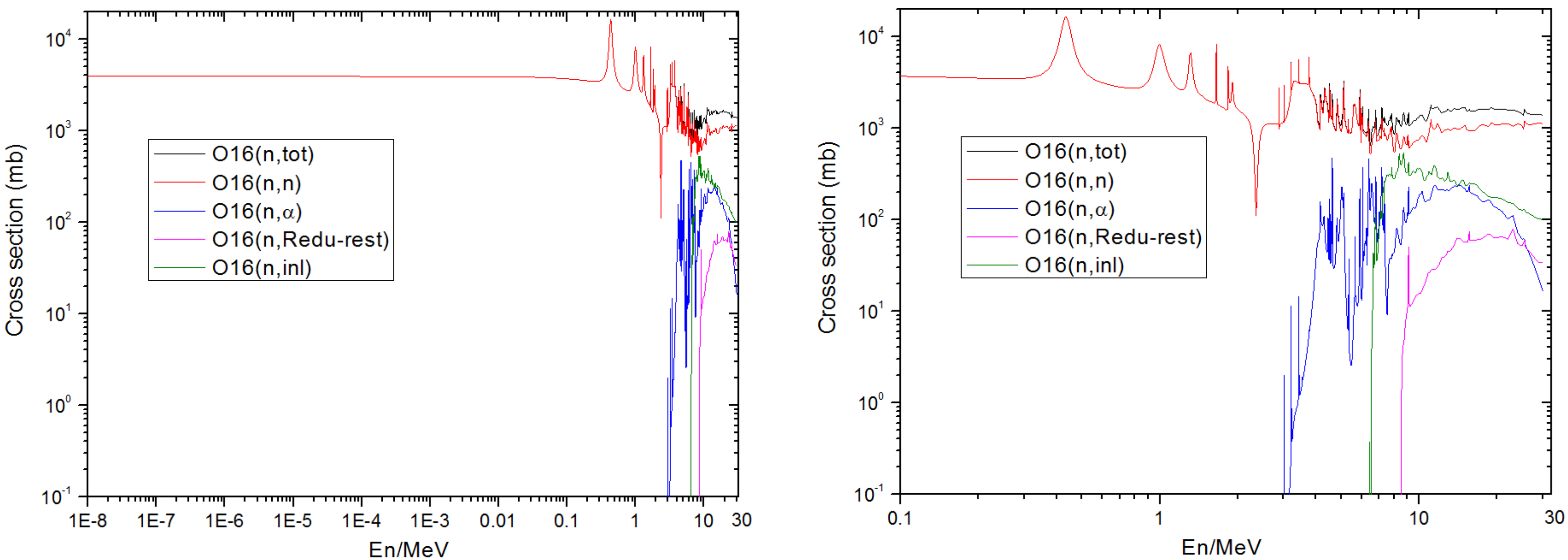

Figure11. The (n, tot), (n, el), (n, inl), (n, α), and (n, Redu-rest),
(n, Redu-rest)=(n,p)+(n,d)+(n,t)+(n,2n)+(n,other)

5 Set of integral C-S calculation values

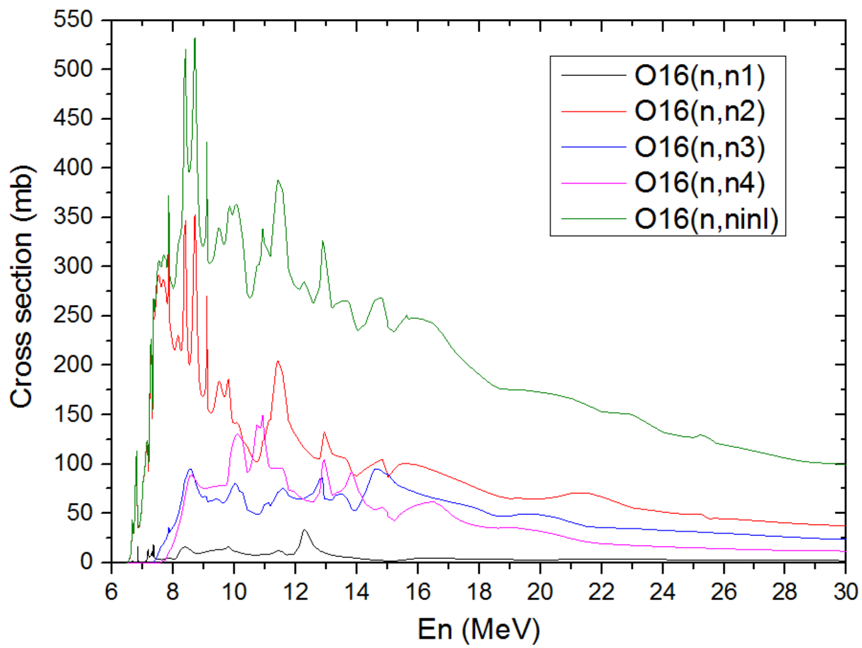

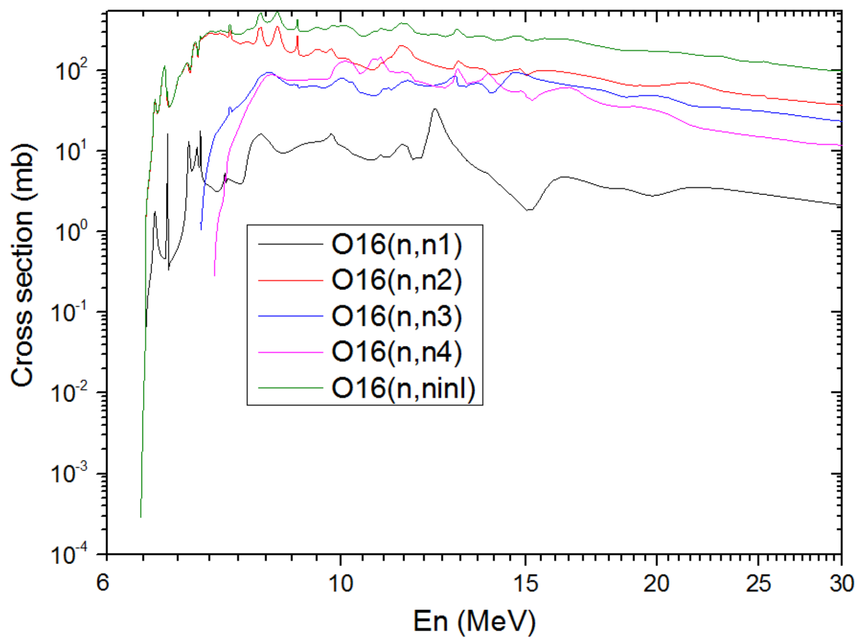

Figure12. The (n, inl), (n, n1), (n, n2), (n, n3), (n, n4), the (n, n2) is much bigger than (n, n1)

5 Set of integral C-S calculation values

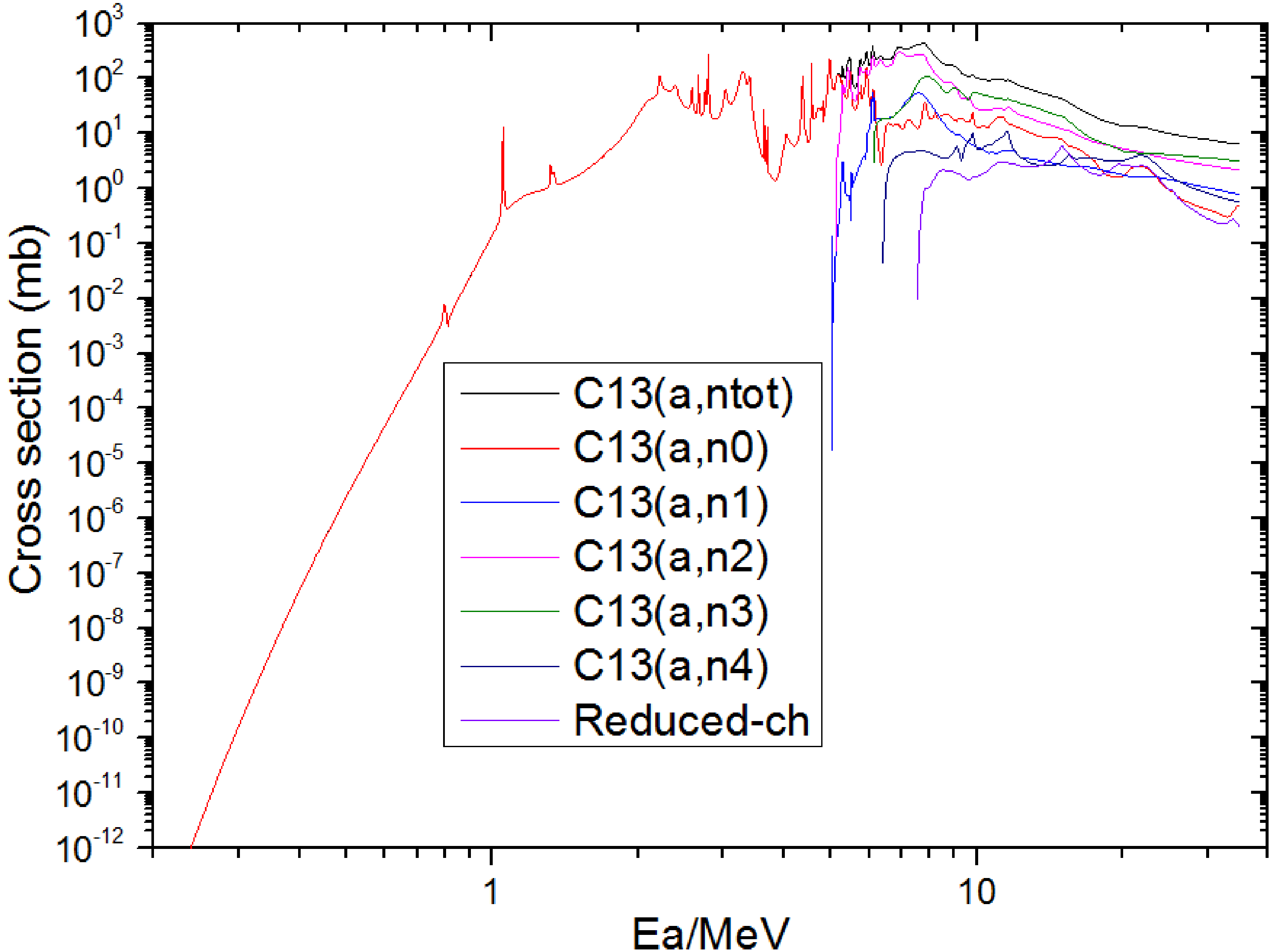

Figure13. The (α, ntot), (α, n0), (α, n1), (α, n2), (α, n3), (α, n4). the (α, n2) is much bigger than (α, n1).

5 Set of integral C-S calculation values

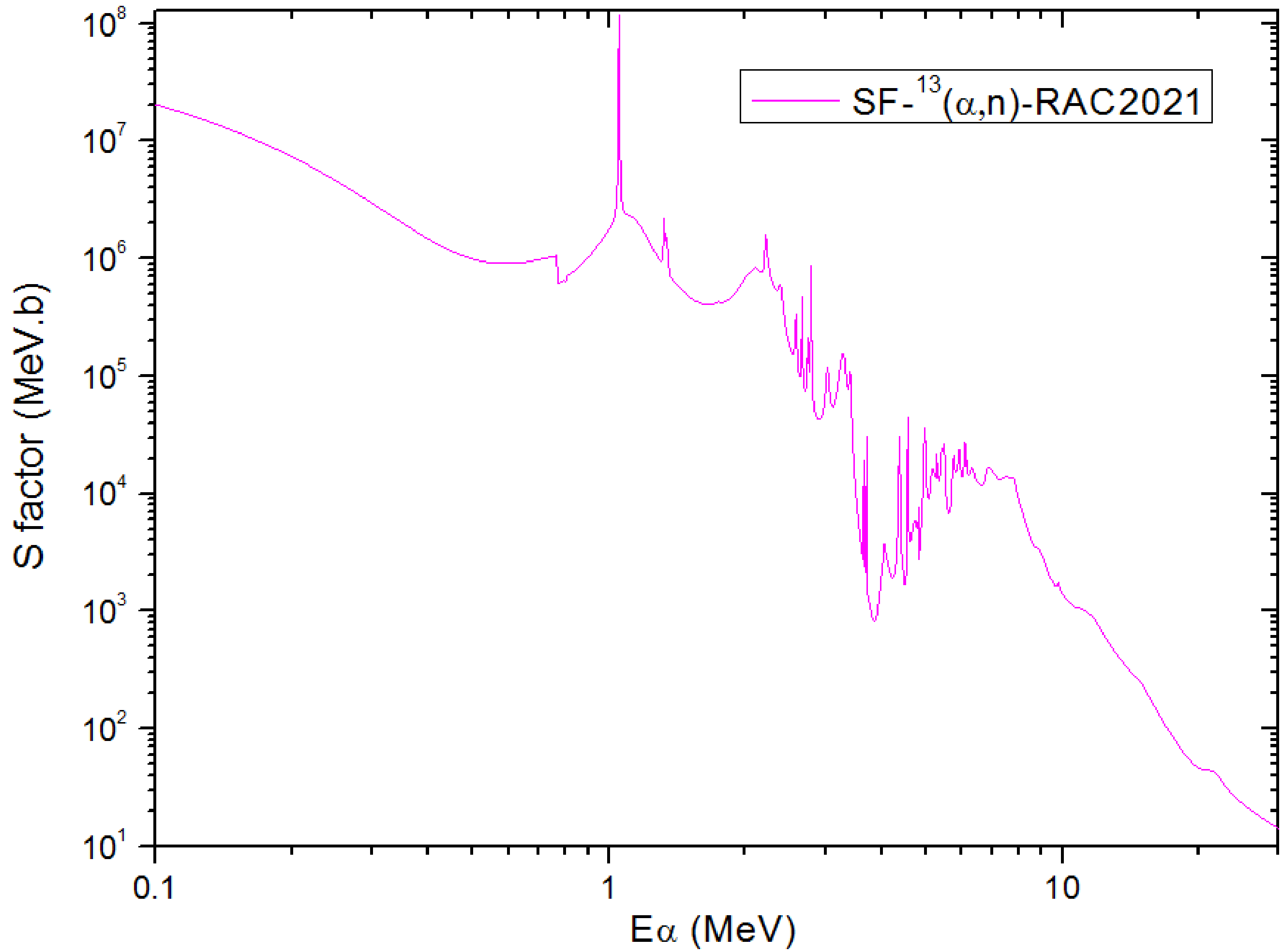

Figure14. The S factor of (α, ntot), it needs improved near 0.8 MeV, which is the junction of two groups of data, and all experimental data have not been normalized.

5 Set of integral C-S calculation values

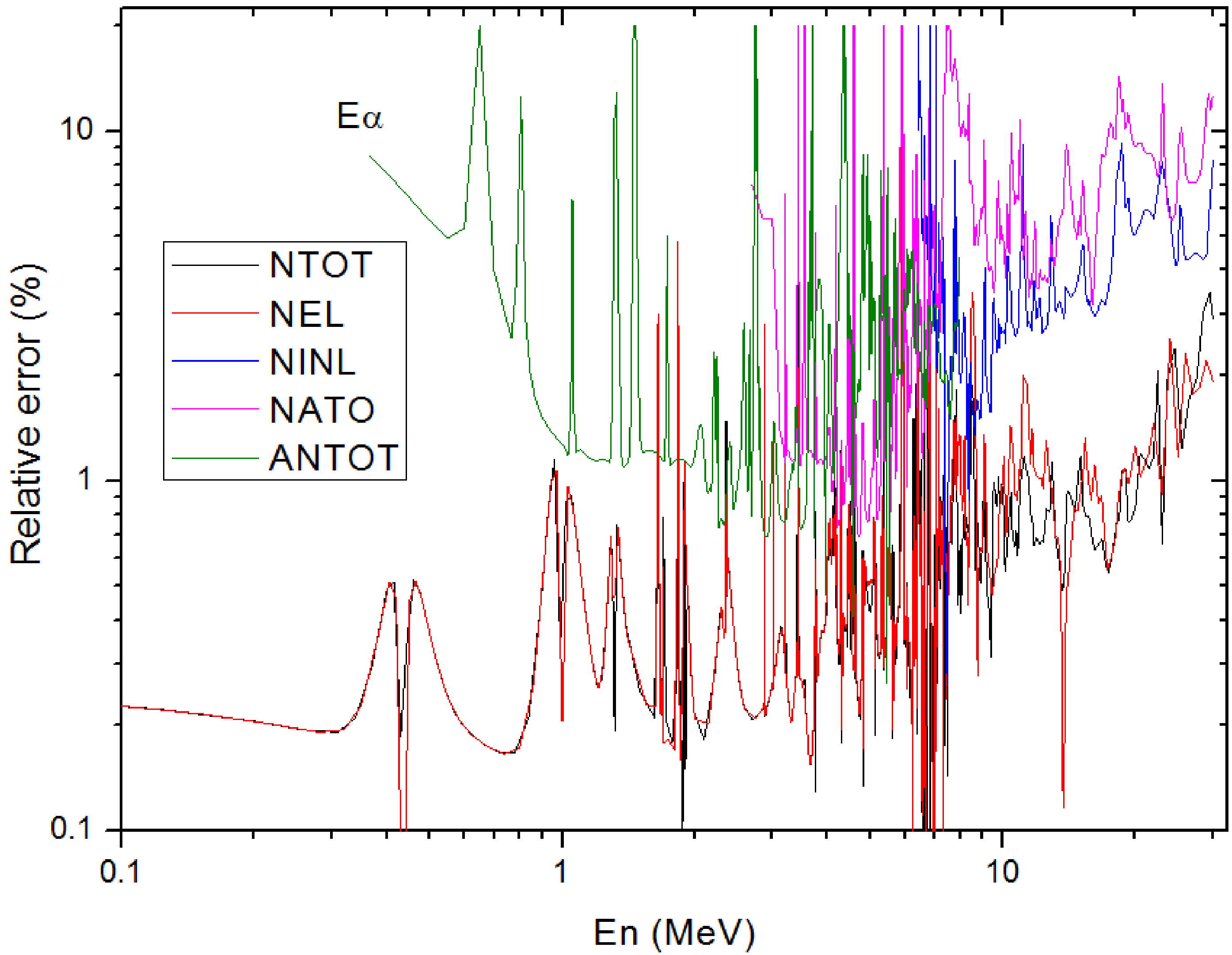

Figure15. The relative error of evaluation values of (n, tot), (n, el), (n, inl), (n, α), and (α, n).

5 Set of integral C-S calculation values

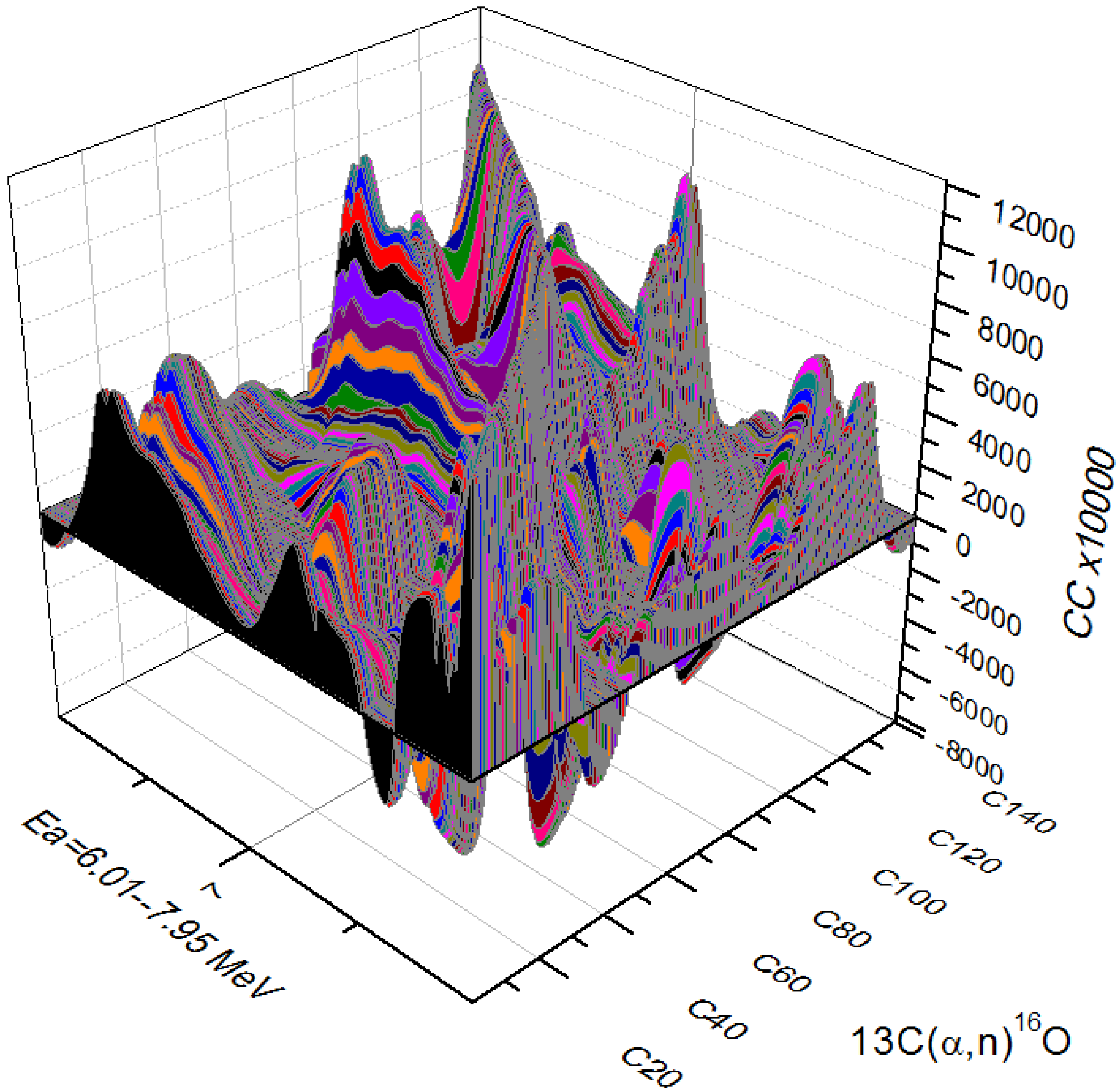

Figure16. The correlation coefficient of (α, n) for *E*α = 6.01 to 7.95 MeV.

6 Discussion

- The evaluation method has been introduced in detail in NDC (NDS)-0791.pdf, and not be repeated here. The main feature of RAC is to adopt the χ^2 expression of 'General Least-Squares' (GLS), instead of 'Approximate Least-Squares' (ALS) which being widely used by now. When GLS was used to fit experimental data at the beginning, χ^2 was relatively large and PPP was easy to occur, which was caused by too large systematic error. In the process of RAC evaluation, the χ^2 (GLS) of GLS and the χ^2 (ALS) of ALS are displayed at the same time. By carefully adjusting the normalization coefficient and reducing the systematic error as much as possible, the χ^2 (GLS) and χ^2 (ALS) are closer and closer, until they are satisfied. In other words, adopting GLS will force the evaluator to carefully normalize the experimental data, so that the experimental data set can achieve a high degree of internal consistency, so as to obtain the most reliable evaluation value.

6 Discussion

- This is a preliminary work. To obtain accurate and reliable (α, n) evaluation value, will need more accurate, reliable, and direct measurement data for (n,n1), (n,n2), (n,n3), (α,n1), (α,n2), (α,n3). Dr. deBoer's data is very important and the reliability of this data set needs to be carefully studied.

Appendix I. Elastic scattering cross section of $^{16}O(n, n)^{16}O$

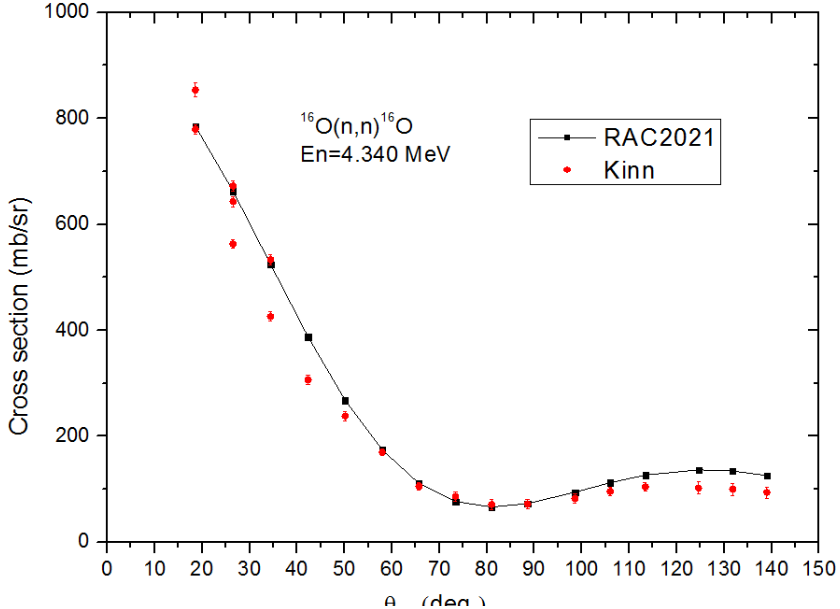

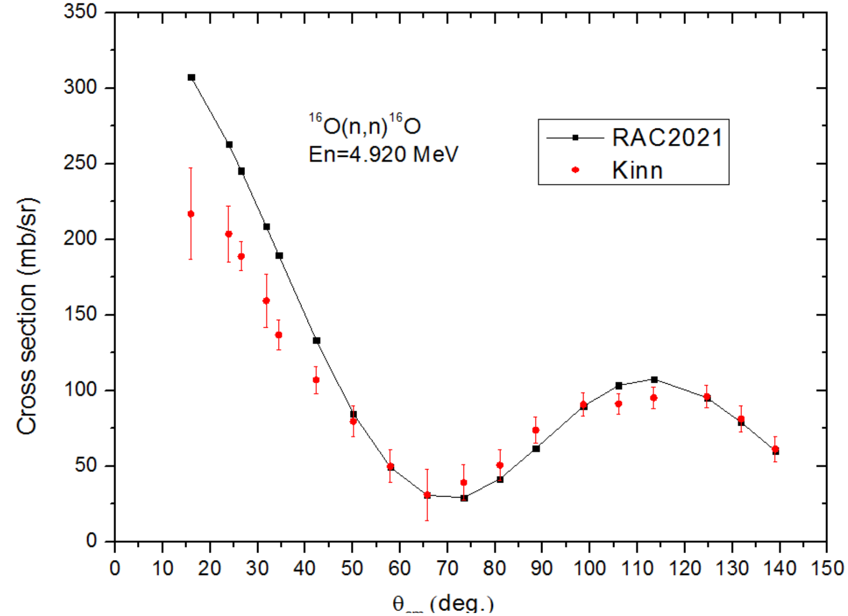

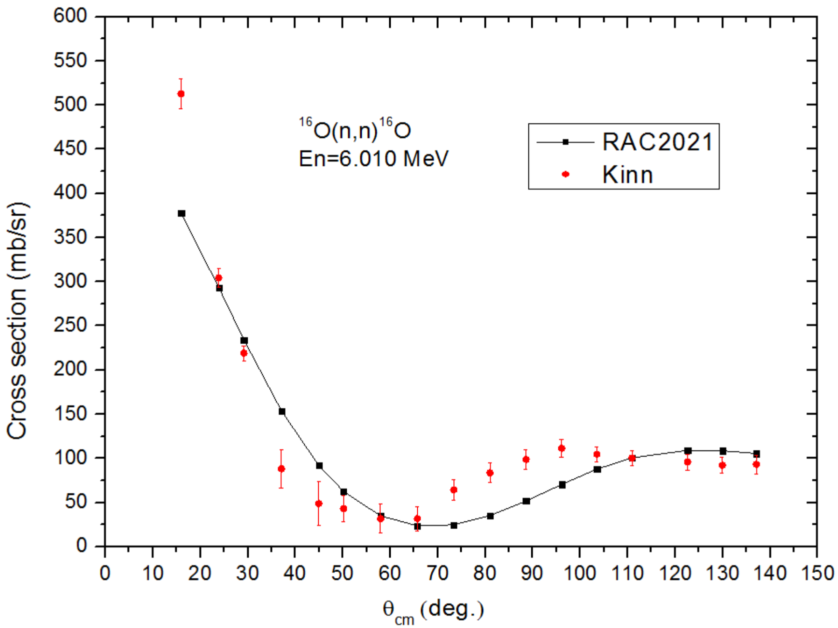

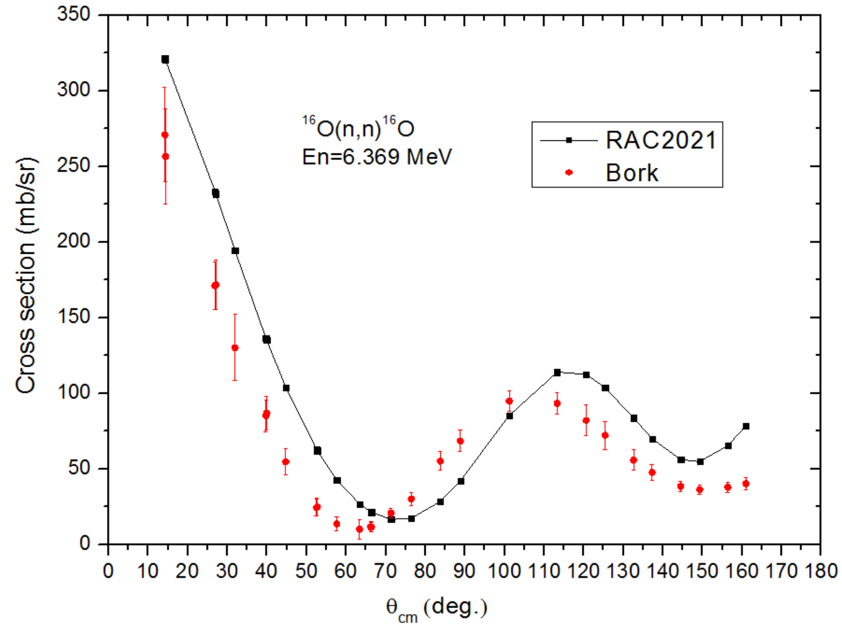

Appendix I. Elastic scattering cross section of $^{16}O(n, n)^{16}O$

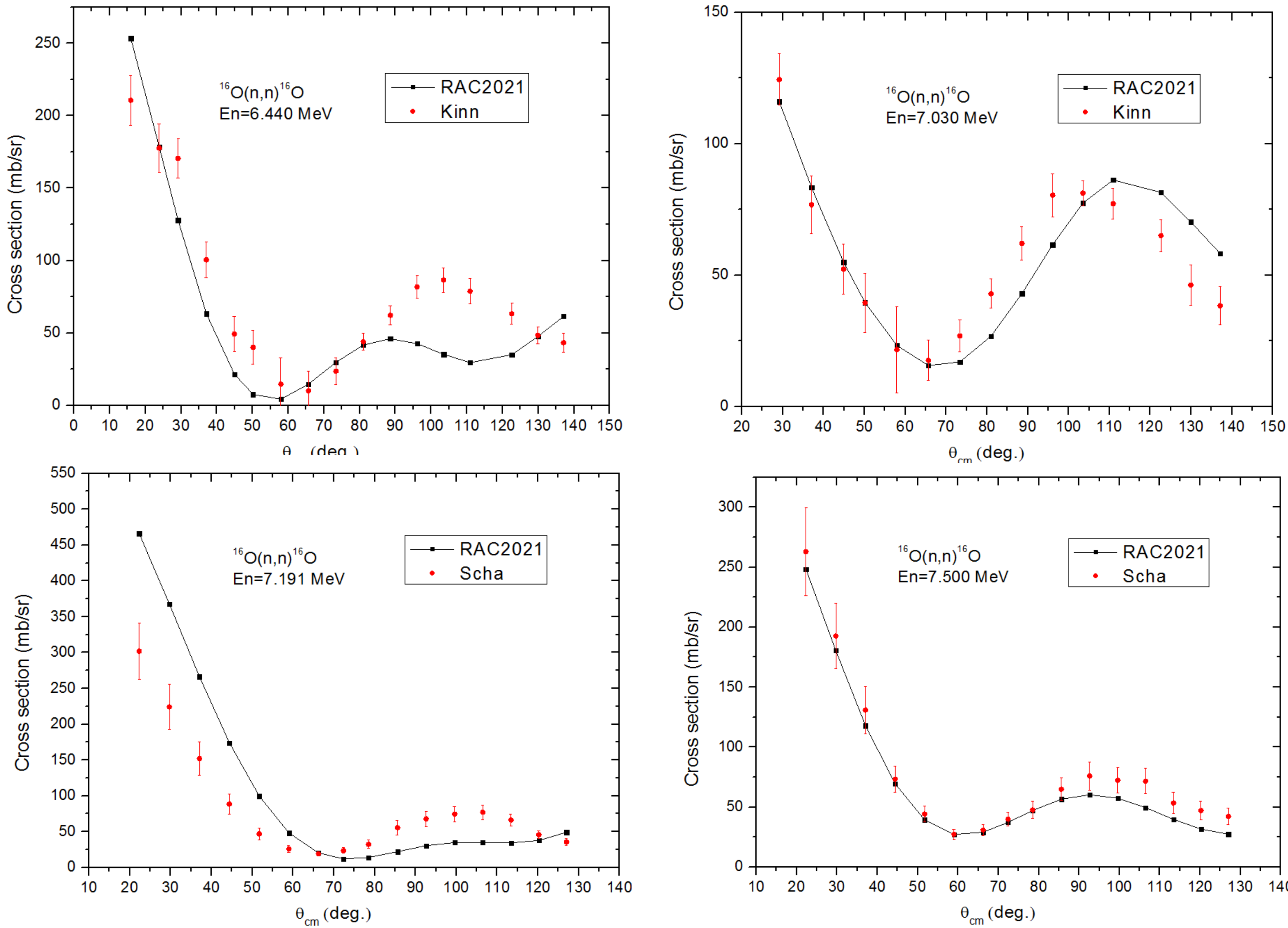

Appendix I. Elastic scattering cross section of $^{16}O(n, n)^{16}O$

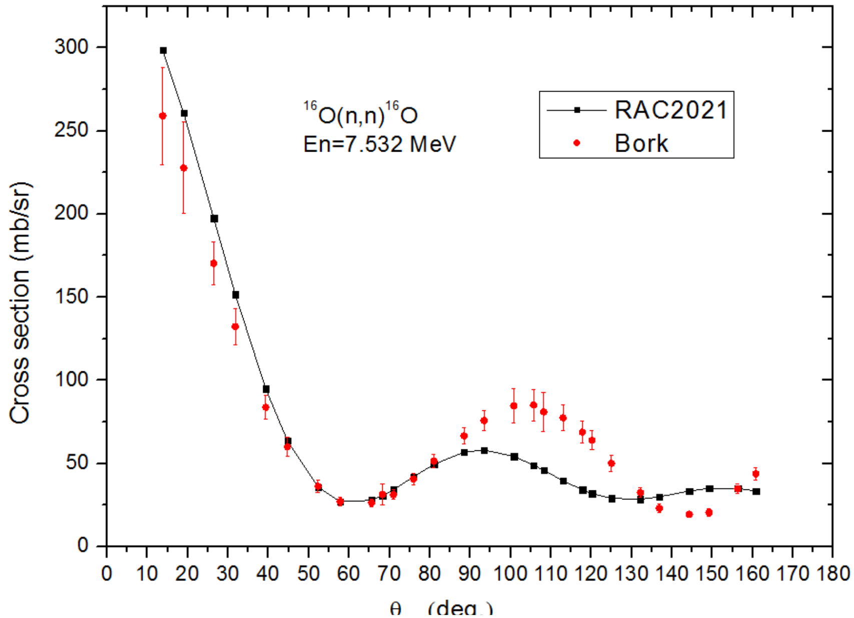

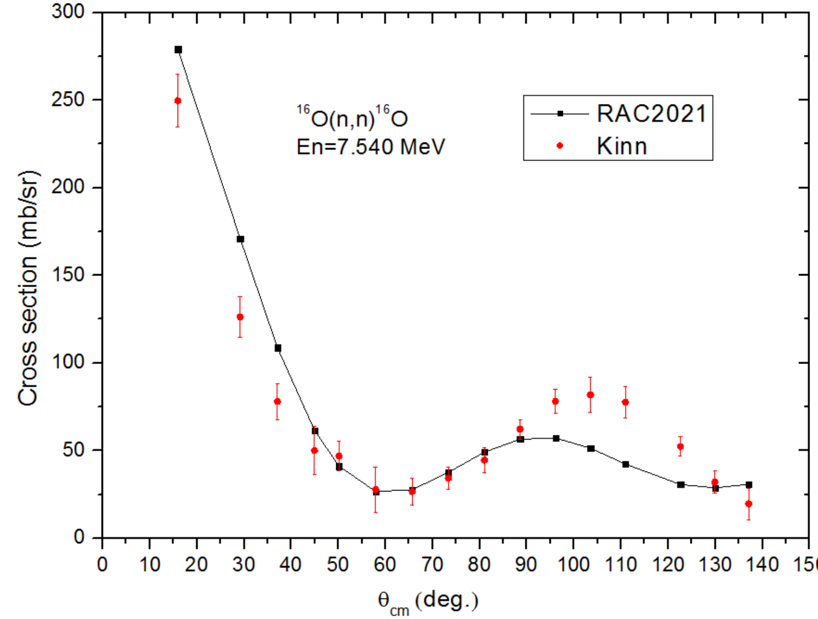

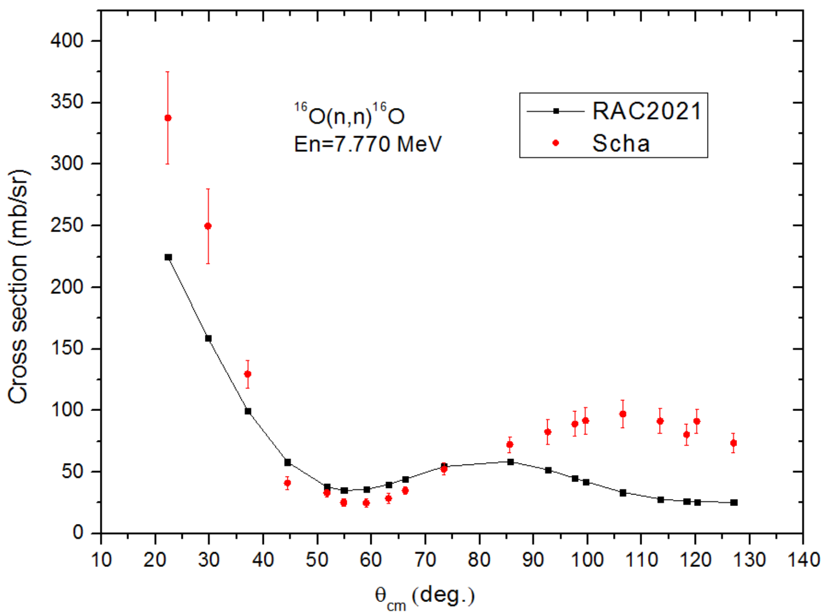

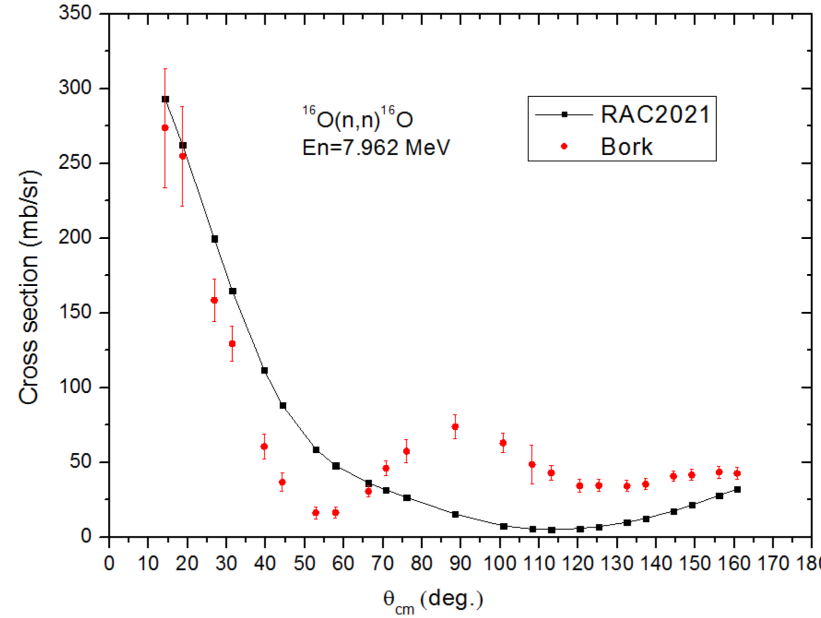

Appendix I. Elastic scattering cross section of $^{16}O(n, n)^{16}O$

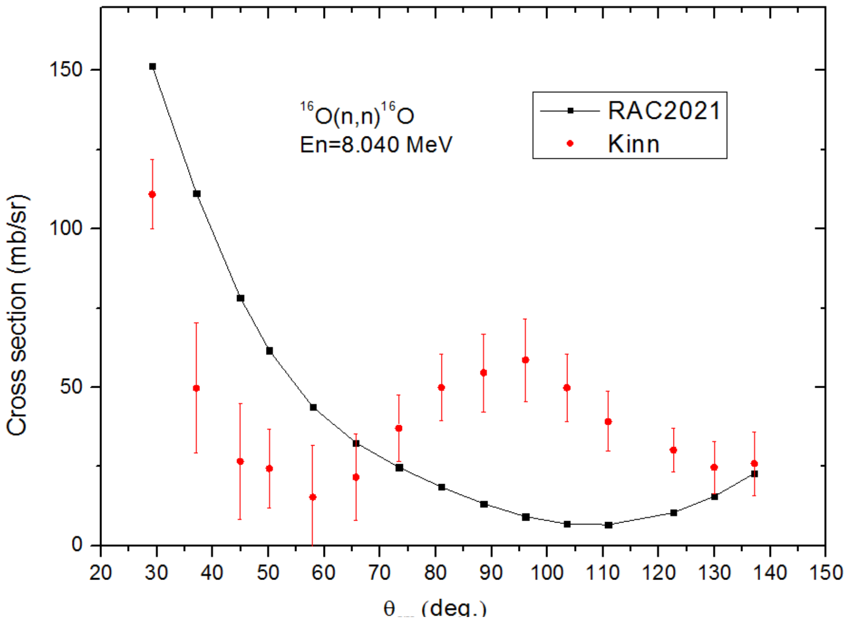

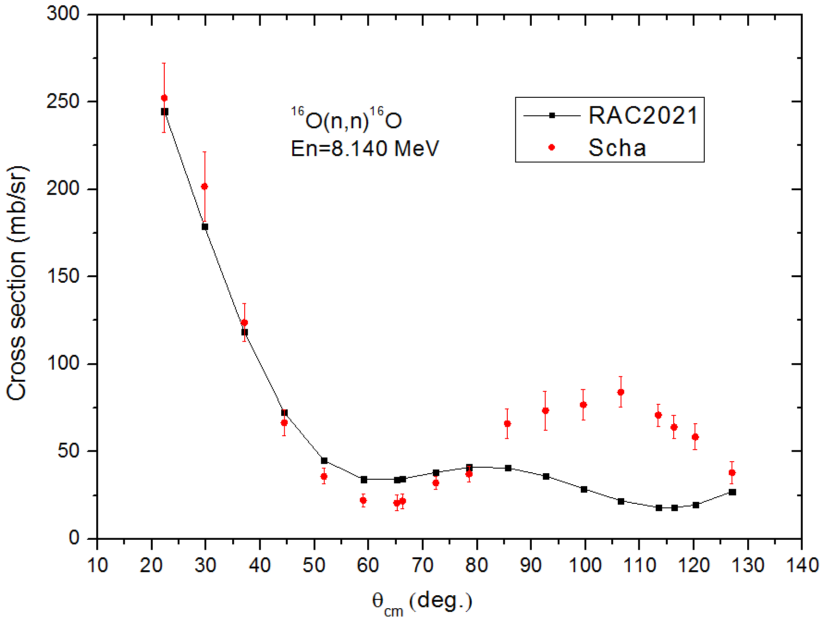

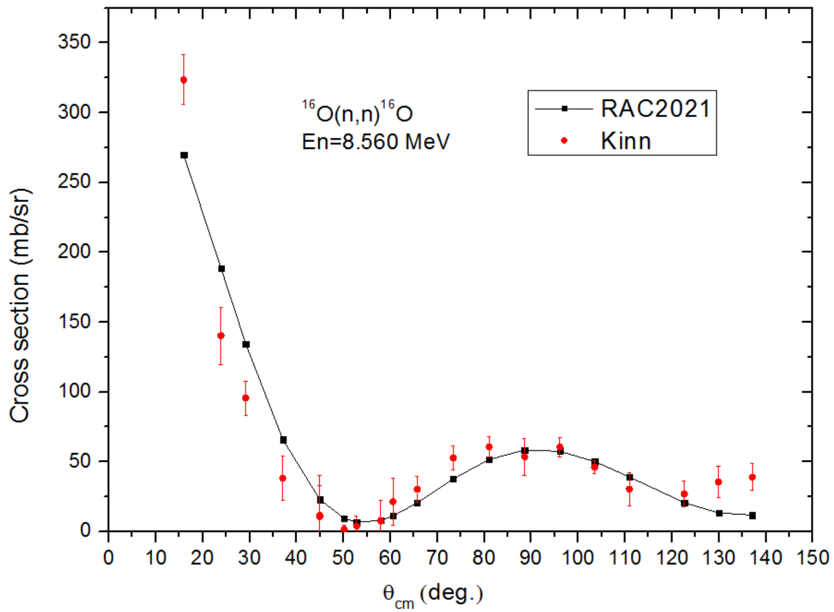

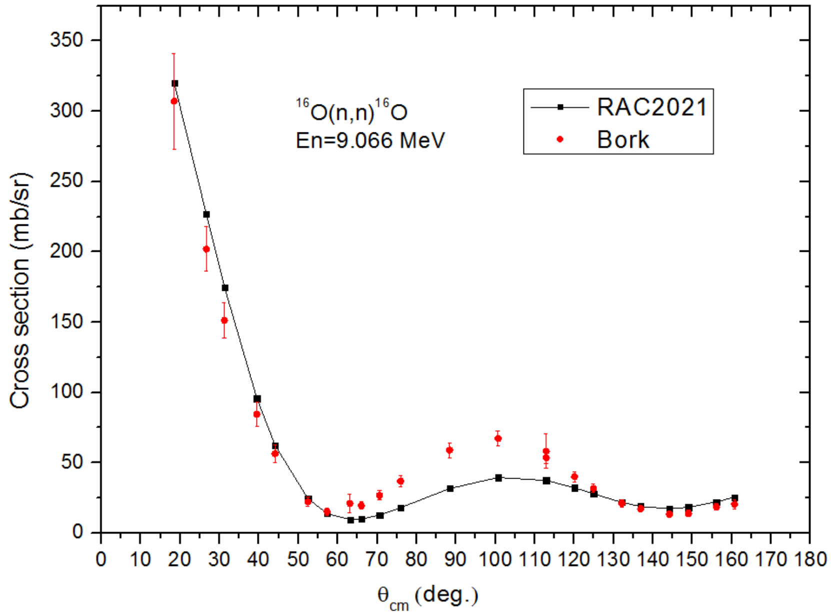

Appendix I. Elastic scattering cross section of $^{16}O(n, n)^{16}O$

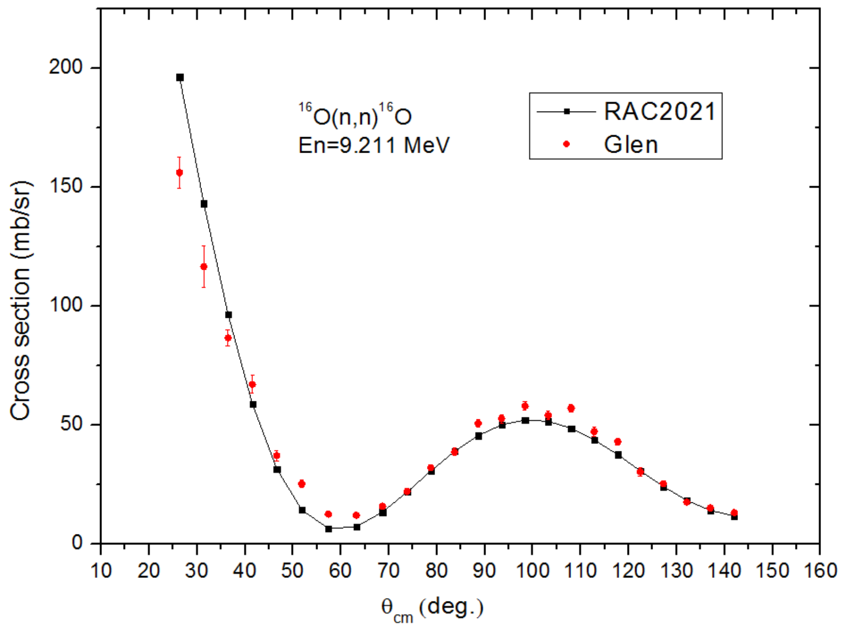

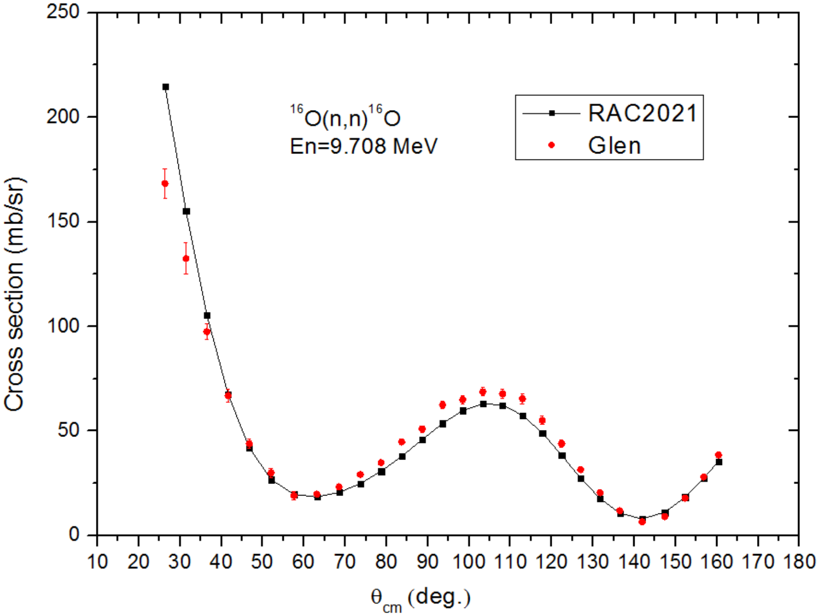

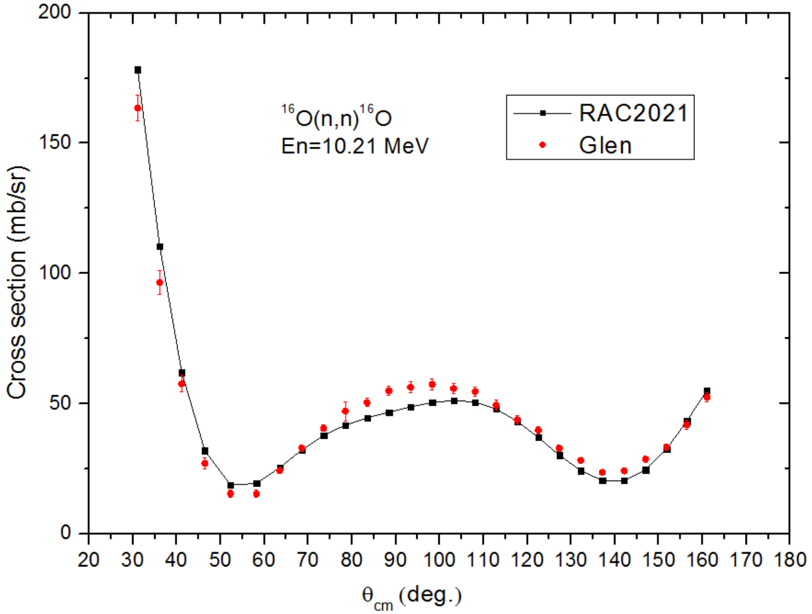

Appendix II. Elastic scattering cross section of $^{13}C(\alpha, \alpha)^{13}C$

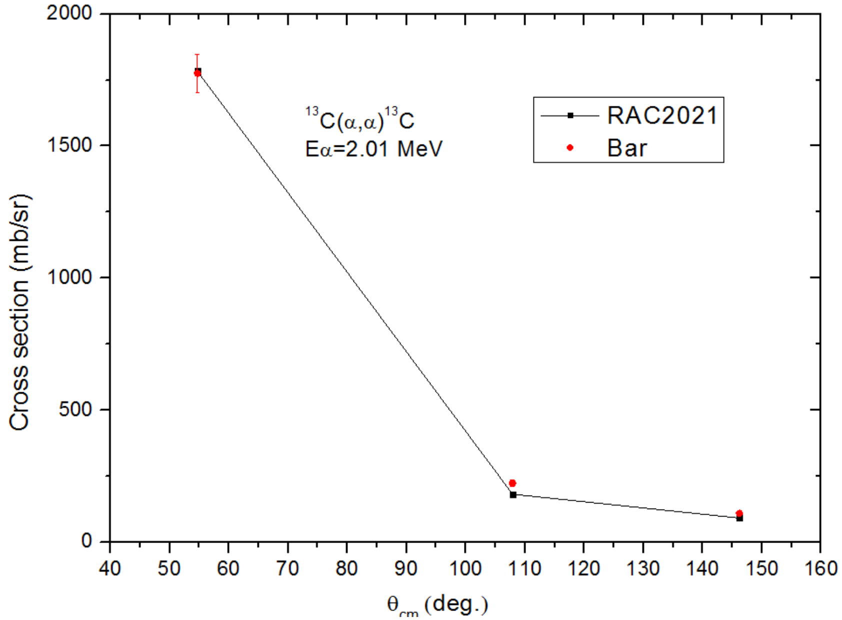

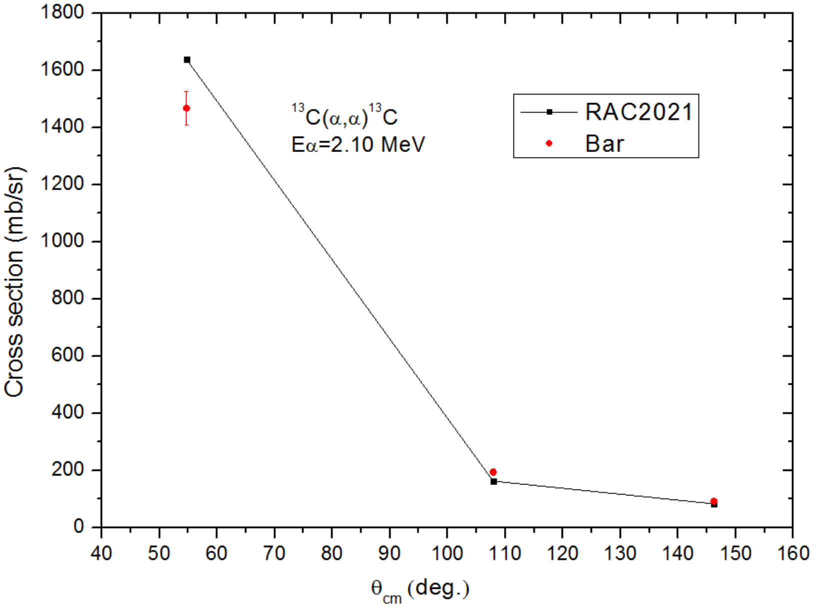

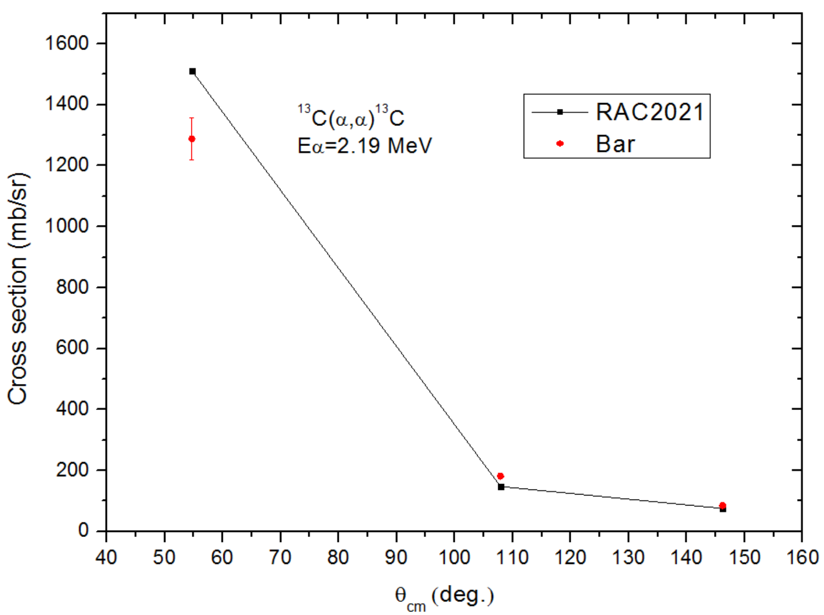

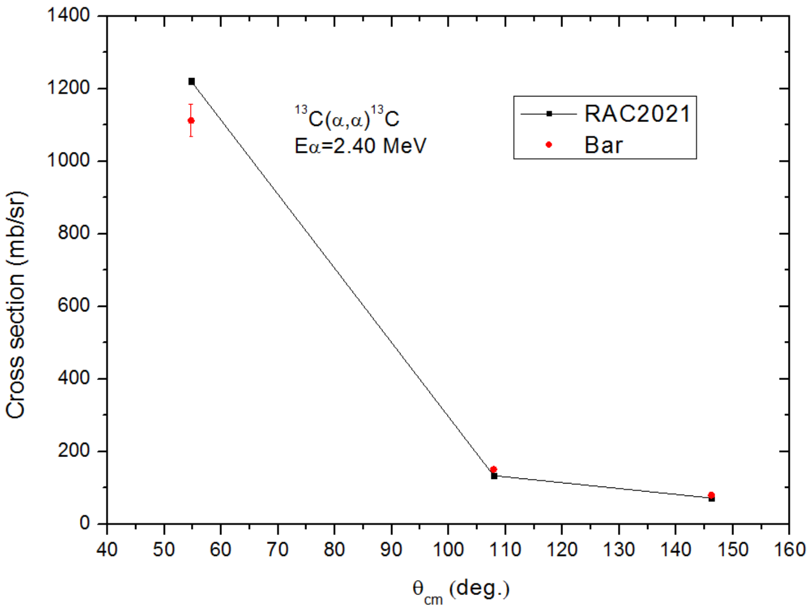

Appendix II. Elastic scattering cross section of $^{13}C(\alpha, \alpha)^{13}C$

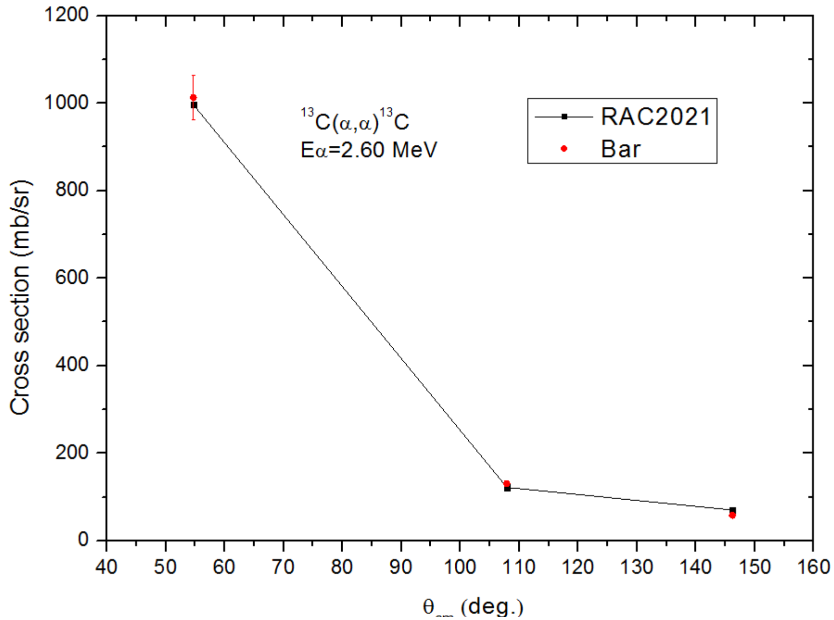

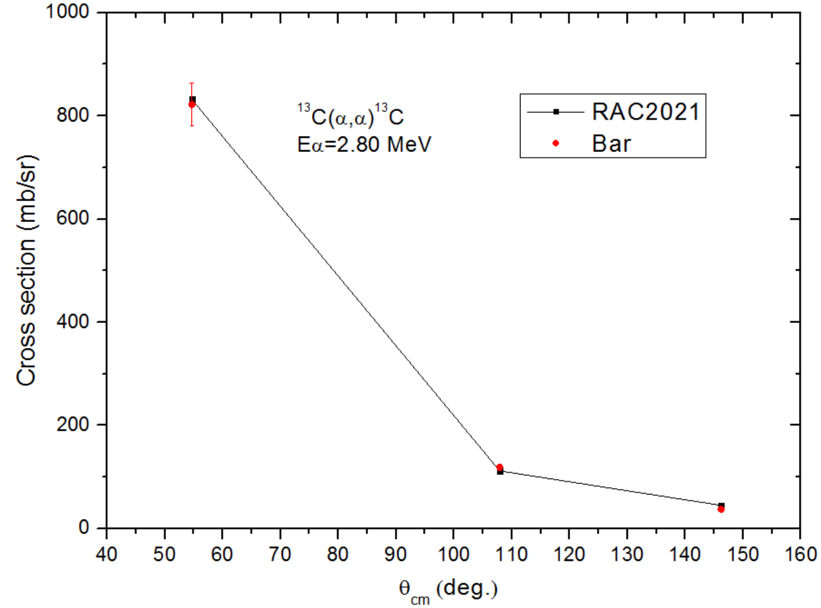

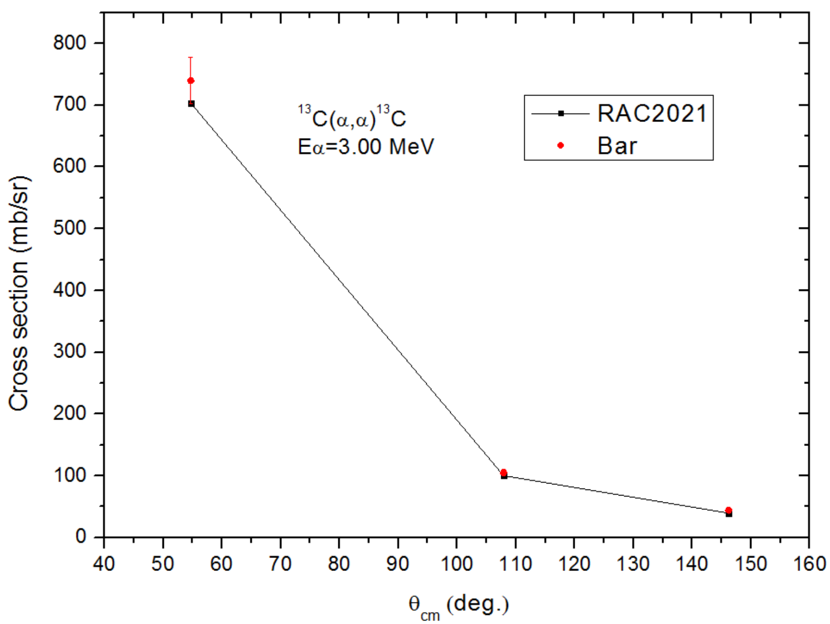

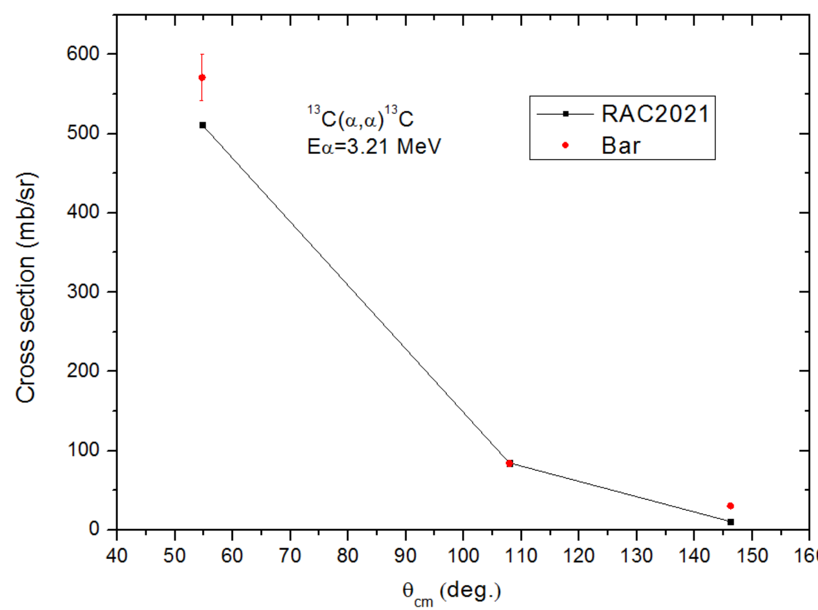

Appendix II. Elastic scattering cross section of $^{13}C(\alpha, \alpha)^{13}C$

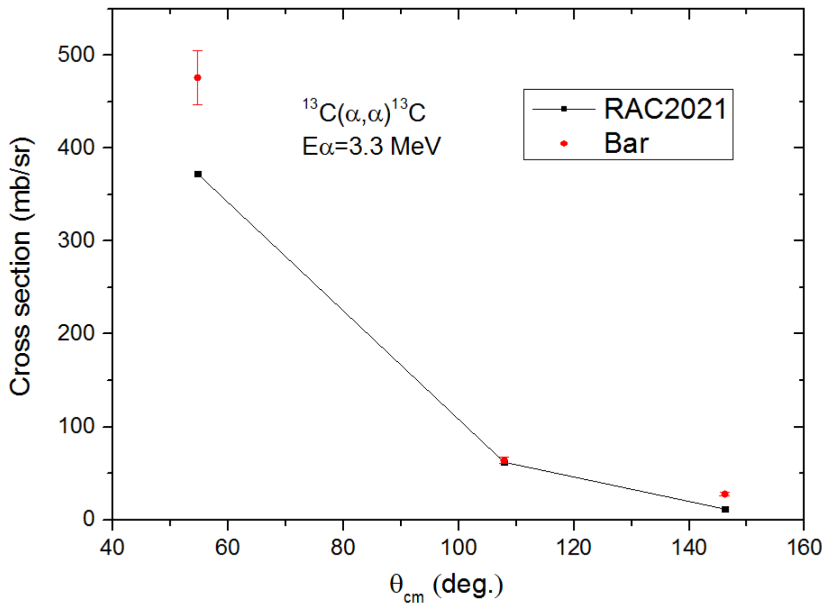

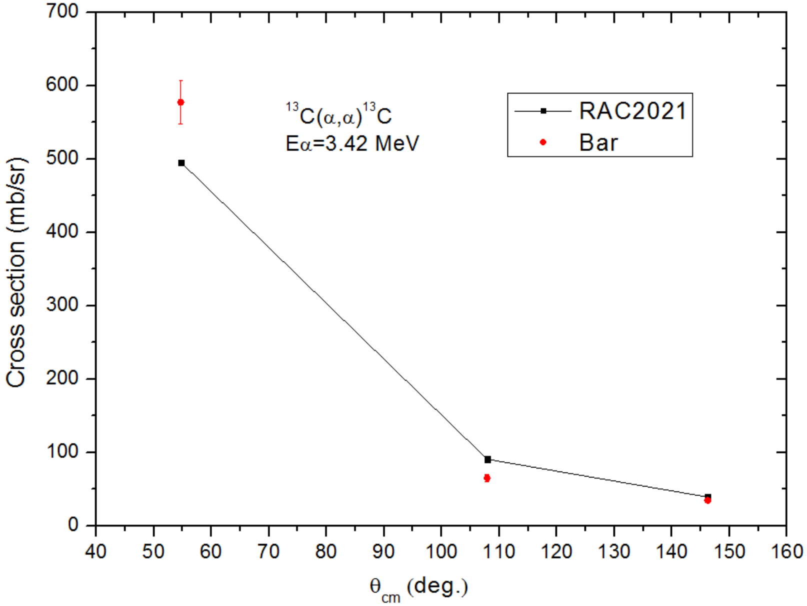

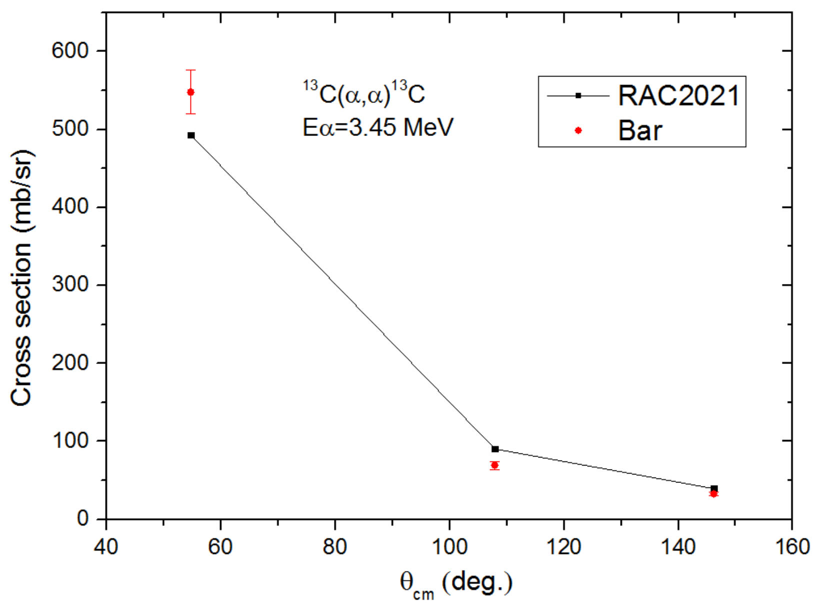

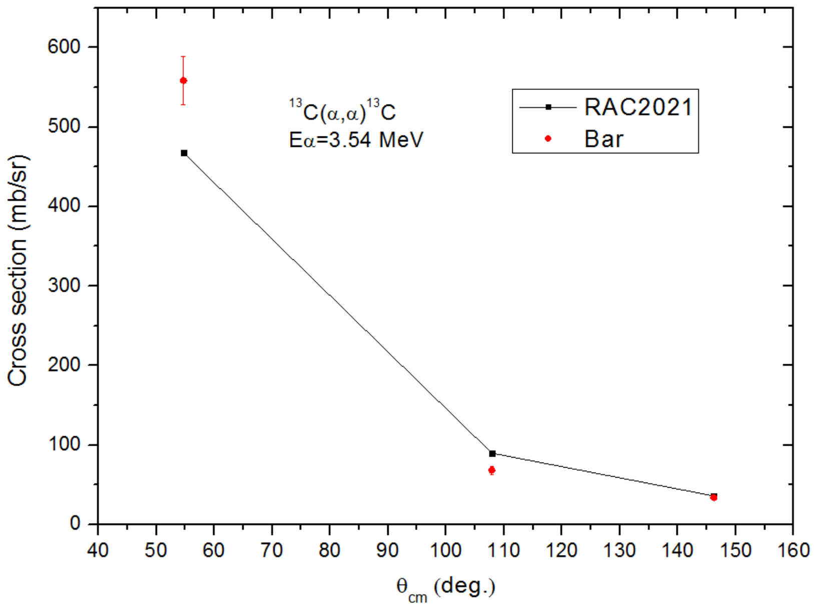

Thanks for your attention!!!